


## RESEARCH ARTICLE

WILEY

# Morphometric properties, scaling laws and hydrologic response of the Greater Paris combined sewer system

Mohamad Achour<sup>1,2,3</sup>  | Nanée Chahinian<sup>1</sup> | Katia Chancibault<sup>4</sup> |  
Hervé Andrieu<sup>4</sup> | Roger Moussa<sup>3</sup>

<sup>1</sup>HSM, IRD, CNRS, Univ Montpellier, Montpellier, France

<sup>2</sup>TVES, Université de Lille, Lille, France

<sup>3</sup>LISAH, Univ Montpellier, INRAE, IRD, Montpellier SupAgro, Montpellier, France

<sup>4</sup>GERS - LEE, Univ Gustave Eiffel, Bouguenais, France

## Correspondence

Mohamad Achour, HSM, IRD, CNRS, Univ Montpellier, France.

Email: [mohamad.achour@univ-lille.fr](mailto:mohamad.achour@univ-lille.fr)

## Funding information

French Research Institute for Sustainable Development (IRD)

## Abstract

Morphometric properties of channel networks are useful tools to classify catchments and calculate their hydrological response. Scaling laws have been established for Optimal Channel Networks (OCNs), which are defined based on a generative geomorphological mechanism of minimizing the total energy dissipation. However, sewer networks obey engineering efficiency rules and are conceived based on local optimizations, both in time and space, for minimal costs. Not all the scaling laws have been verified for artificial sewer networks found in urban areas. This raises questions regarding the applicability of OCN scaling laws to sewer networks and their potential impact on the shape of the Geomorphological Instantaneous Unit Hydrograph (GIUH). Hence, this work aims to study the morphometric properties of the Greater Paris combined sewer system through a case study on twelve nested subcatchments. A two-step methodology is used. First, the morphometric properties are analysed using the reference Horton-Strahler, Rodríguez-Iturbe and Moussa-Bocquillon scaling laws. The results show that Horton-Strahler's laws of bifurcation are verified while the length and area laws are not always verified. Rodríguez-Iturbe and Moussa-Bocquillon laws are verified with slightly different values of the descriptors in comparison to OCNs. Second, these morphometric properties are used to calculate four GIUHs: the reference Width Function ( $G_{WF}$ ), the Nash unit hydrograph ( $G_N$ ) using Horton-Strahler ratios, the Nash Unit Hydrograph equivalent ( $G_{Ne}$ ) using Moussa-Bocquillon descriptors, and the Hayami function ( $G_H$ ) solution of the diffusive wave equation. We identified four catchments for which the scaling laws are verified and therefore all GIUHs are similar while for four other catchments the scaling laws are not verified and strongly impact the GIUHs. These morphometric descriptors and the GIUHs can be considered as 'hydrological signatures' of Combined Sewer Systems (CSSs) and are useful for the comparison and classification of hydrological responses.

## KEYWORDS

combined sewer system (CSS), GIUH, Horton-Strahler laws, power law, urban network

This is an open access article under the terms of the [Creative Commons Attribution](https://creativecommons.org/licenses/by/4.0/) License, which permits use, distribution and reproduction in any medium, provided the original work is properly cited.

© 2023 The Authors. *Hydrological Processes* published by John Wiley & Sons Ltd.

## 1 | INTRODUCTION

The organization of a river network is hypothesised to impact many processes such as catchment response during floods (Rodríguez-Iturbe et al., 1979), erosion (Dietrich et al., 1993; Raff et al., 2003), metabolism of organic carbon (Battin et al., 2008; Bertuzzo et al., 2017; Coble et al., 2019) as well as river's biogeochemistry (Wollheim et al., 2018) and biodiversity patterns (Muneepeerakul et al., 2019; Rodríguez-Iturbe et al., 2009). Morphometric descriptors, which are physical and geometric coefficients and ratios of the catchment, are useful tools to classify channel networks, analyse their morphometric properties and calculate the Geomorphological Instantaneous Unit Hydrograph (GIUH) (Gupta et al., 1980; Rodríguez-Iturbe & Valdés, 1979). The GIUH links the unit hydrograph routing theory based to the catchment's geomorphological features (Gupta et al., 1980; Rodríguez-Iturbe & Valdés, 1979). Thus, morphometric descriptors could be very useful in regions where no field data is available to calculate catchment hydrological response (Hrachowitz et al., 2013). This will enable managers to assess the network's impact on flood dynamics, water quality or ecological status.

The quantitative study of channel networks' architecture began with Horton's (1945) and Strahler's (1957) attempts at classifying channels by orders. Later, Tokunaga (1978) put forward a new classification method. The advent of Digital Elevation Models (DEM) saw the emergence of new approaches to extract hydrographic networks from DEMs and characterize their structure. Following the pioneering work of Rodríguez-Iturbe and Valdés (1979), Horton-Strahler's ratios were incorporated into the theoretical scheme of the GIUH (Gupta et al., 1980; Rosso, 1984). Moreover, on the basis of fractal properties of channel networks, Rodríguez-Iturbe and Rinaldo (1997) established the scaling laws known as the exceedance probability distribution of cumulative drainage area. They showed its fractal property for natural networks. These networks are created based on the principle of minimizing the total energy dissipation and are also known as Optimal Channel Networks (OCN). To overcome some limitations of the Horton-Strahler properties, Moussa and Bocquillon (1996) and Moussa (2003, 2009) put forward new power laws function of the drained area, which are useful to classify the internal nodes of the channel network, and establish the relationship between the shape of the network and the GIUH. All these approaches are complementary and aim to characterize the links between the morphometric properties and the corresponding hydrological response of channel networks.

Optimal Channel Networks (OCNs) are defined based on a generative mechanism of minimizing the total energy dissipation (Paik & Kumar, 2008). Sewer networks on the other hand obey engineering efficiency rules and are conceived based on local optimizations, both in time and space, for minimal costs (Yang et al., 2017). While network design may initially focus on local considerations, the long-term operation of the system requires global adjustments as it processes and repairs the localized failures that arise during its growth. This trajectory leads the system towards a state of global functionality, often characterized as an "optimal configuration." Yang et al. (2017) showed that at the smallest scales engineering design and local constraints dominated,

but over time as the networks grew in size their scaling properties tended to converge towards that known for river networks.

Several studies have evaluated scaling laws, Yang et al. (2017) among others, including accumulated drainage area exceedance probability, and Hack's Law. They showed that for the smallest catchments (<2 km<sup>2</sup>), length-area scales linearly, but power law scaling emerges as the urban drainage network grows. While accumulated drainage area exceedance probability plots for river networks are abruptly truncated, those for urban networks present a temporal evolution of the scaling relationships. Although scaling laws and morphometric properties have been established for OCNs, they are not necessarily verified for artificial channel networks in urban areas. Therefore, questions may arise as to (i) whether the scaling laws established for OCNs may also be true for non-OCN artificial channel networks, (ii) what their values are and how they vary in comparison to OCNs. If these laws are verified, a third question may arise on how they may impact the shape of the GIUH and whether specific GIUHs can be established for artificial channel networks. Indeed, the overwhelming majority of research available in the literature has focused on natural hydrographic networks where the slope is the driver of flow and geomorphological organization (Ibbitt, 1997; Moussa et al., 2011; Raff et al., 2003; Rinaldo et al., 1992; Tarboton, 1996). In comparison, very few applications were carried out on anthropogenic channel networks such as those of urban (Jovanovic et al., 2019; Meierdiercks et al., 2010; Rodriguez et al., 2005) or agricultural areas (Hallema & Moussa, 2014). Although scaling laws and morphometric properties have been established for OCNs, not all laws have been verified for artificial channel networks in urban areas. Yang et al. (2017) have shown that Hack's law and the power law are verified for separate wastewater networks (i.e., not combined with storm water). Zischg et al. (2019) have shown that the urban drainage network of Innsbruck (mainly combined sewer) follows a truncated Pareto power law. Their results also showed that at early stages of growth, sewer networks tend to deviate from the scaling laws of rivers. However, as they grew in size the scaling laws tend towards those seen in rivers and are eventually indistinguishable from rivers. Krueger et al. (2017) on the other hand have analysed the evolution of the sewer system of a large Asian city and have shown power-law characteristics in the network throughout the analysis period (1970–2005). The authors state that when an urban network is laid, its topology is similar to that of river networks and have different factors forcing their evolution, their layout is not random. Some studies have looked into the fractal structure of urban networks (Gires et al., 2015, 2017 and 2018) but fewer studies have looked into the morphometric properties of combined sewer systems (CSS) which collect urban stormwater and wastewater in the same network of pipes (McGrath et al., 2019). CSSs are in use in many countries around the world (Botturi et al., 2021; Kvitsjøen et al., 2021; Munro et al., 2019; Nickel & Fuchs, 2019).

CSS networks are usually designed to favour gravity fed flow, but their morphology also depends on several factors: the urban development over time, the street network morphology as sewer pipes are often located below streets and the location of the treatment plant to which the CSS conveys urban water. Local topographic constraints,

increasing consumer demands, new management practices and environmental requirements may impose additional constraints. Thus, the network's structure may be impacted by other decision rules than just maintaining adequate slope values to insure gravity flow. Moreover, a major difficulty lies in the lack of digitized data on sewer networks for small and mid-sized towns. This calls for the development of adequate procedures to define these networks.

The objective of this work is to study the morphometric properties of CSSs using the afore-mentioned methods on the sewer network managed by the Greater Paris Sanitation Authority (SIAAP-Syndicat Interdépartemental pour l'Agglomération Parisienne). The methodology consists in first defining the morphometric properties of channel networks to compare them to the values reported in the literature for OCNs. The corresponding GIUHs are then computed and compared to each other. The paper is organized in four sections: The first presents the study site. The morphometric properties and scaling laws of the Greater Paris CSS are presented in the second section. In section three, a hydrological use case is presented where the morphometric properties are used to derive GIUHs. The fourth section deals with the conclusions drawn from this work and the new perspectives it offers. Appendix A shows the list of notations and Appendix B details

the procedure developed to extract the network characteristics of the Greater Paris CSS. A Data S1 section is joined to this article with all detailed results on the 12 subcatchments of the Greater Paris CSS.

## 2 | THE STUDY SITE: THE GREATER PARIS COMBINED SEWER SYSTEM (CSS)

The sewer system is managed at the Greater Paris scale (City of Paris and the three surroundings departments Hauts-de-Seine, Seine-Saint-Denis et Val de Marne). It covers a total urban area of 1800 km<sup>2</sup> and serves 9 million inhabitants treating 2.5 million 125 m<sup>3</sup> of wastewater daily in dry weather across 180 municipalities (<https://www.siaap.fr/siaap-greater-paris-sanitation-authority/>). The part of this sewer network which drains the City of Paris and the older urban areas consists of a combined sewer system (hereafter CSS) which collects both sanitary sewage and stormwater runoff in a single-pipe. The more recent part of the sewer network consists of a separate sewer network, mainly located in the outlying areas. The Greater Paris network presents a significant complexity and intersections between CSS, wastewater and stormwater networks, with also downstream

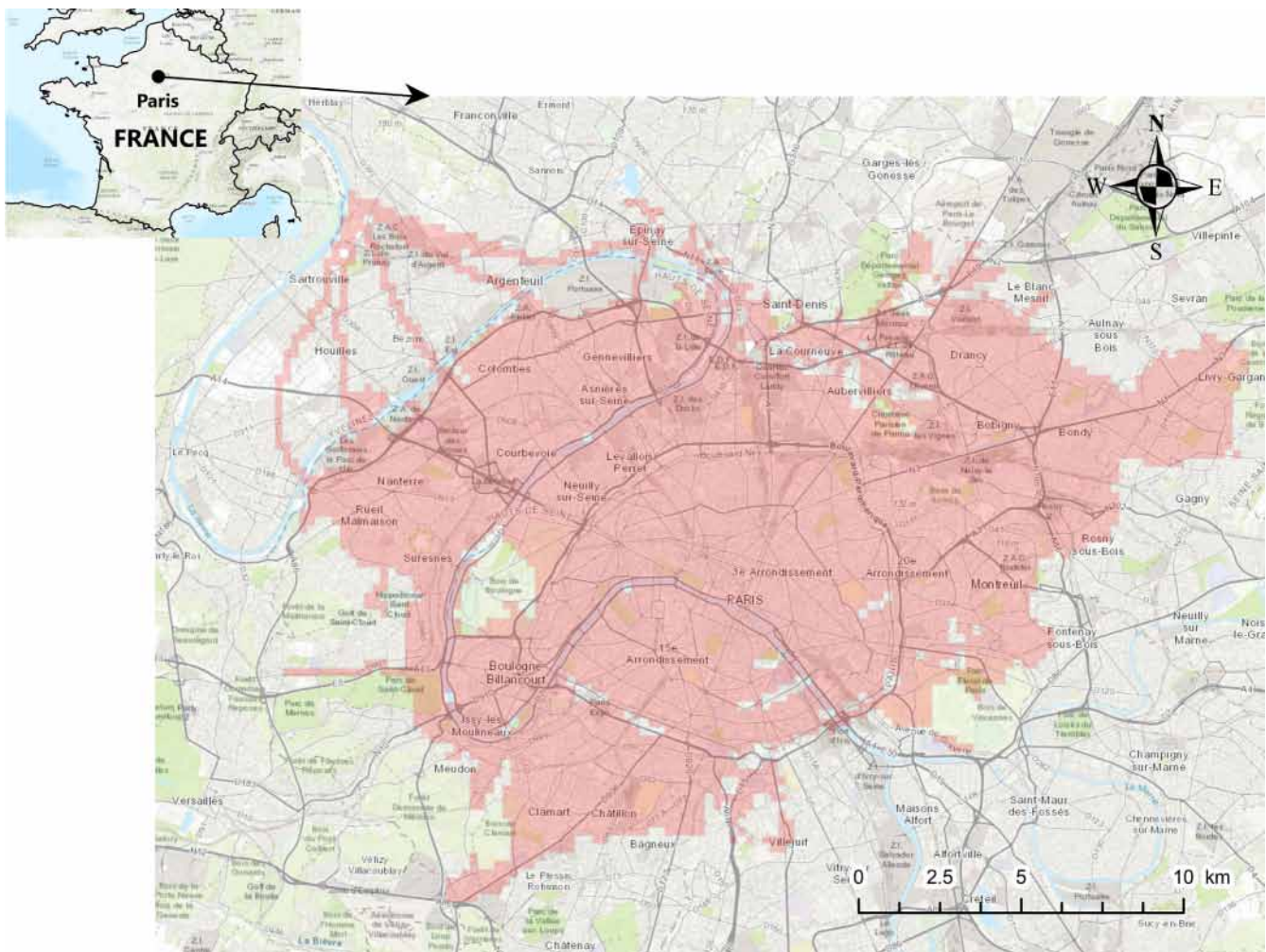


**FIGURE 1** Limits of the study area of the Greater Paris combined sewer system.

outlets. In this project, only the CSS is studied. The study area (Figure 1, area in red) covers only the area drained by CSS: a total area of 310 km<sup>2</sup>.

A reconstructed version of the Greater Paris sanitation network was provided by Chancibault et al. (2020) based on the real network data provided by SIAAP, the City of Paris and the three departments of the study area (Figure 2). Unfortunately, urban data banks locating

the pipes, when they are not used for the daily management of the sanitation system, present many gaps and topological discontinuities. The catchment map corresponding to the reconstructed network is based on a 250 m-resolution regular grid. Each junction of the network drains the cell that intersects it, while for the cells that do not intersect a junction, a geometric method implemented in ArcGis (Average Nearest Neighbour) is used that allows the cells to be

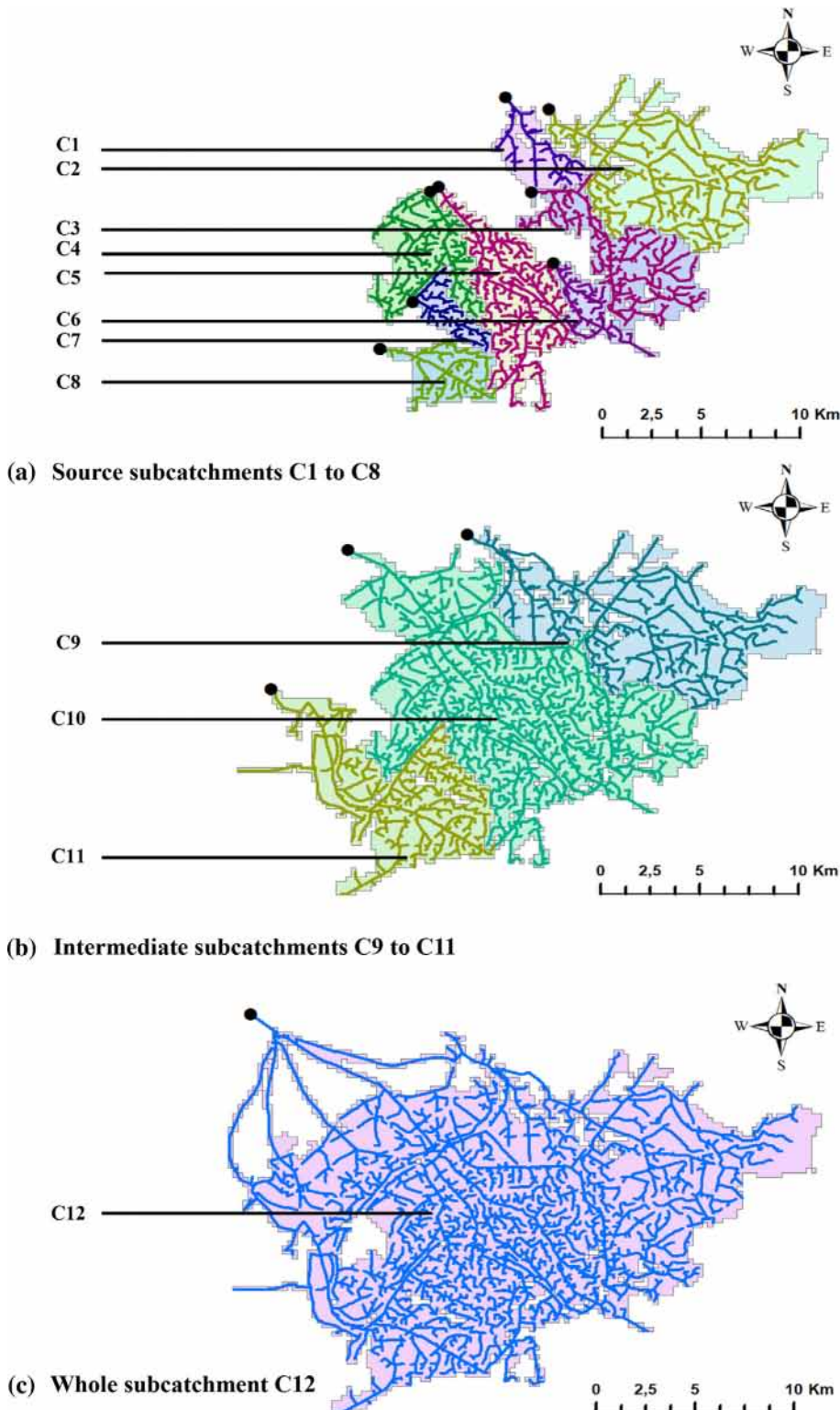


**FIGURE 2** Greater Paris combined sewer system catchments: C1 to C8 are source subcatchments (a), C9 to C11 are intermediate subcatchments (b), and C12 represents the whole catchment (c).

drained to the nearest junction, according to the slope. To solve the problem of intersections, the network has been modified in some places: some segments are eliminated to ensure a single drainage direction in the network; these segments present 0.4% of the total number of segments. In order to choose the segments to be eliminated, several discussions were carried out with the Parisian network operator to determine the main direction and the main flow segments of the network. The network extraction procedure for the Greater Paris CSS is presented in Appendix B.

The study area is lineated by different catchments and subcatchments. The whole drained area by the CSS, flowing to the main Wastewater Treatment Plant WWTP Seine aval constitutes the C12 catchment, where the total length of the channel network is 909 km. It is divided in 11 subcatchments (Figure 2) such as subcatchment C9 includes (C1 and C2), C10 includes (C3 to C6), C11 includes (C7 and C8). Catchment areas range from 8 km<sup>2</sup> (C7) to 310 km<sup>2</sup> (C12) and total channel network lengths from 23 km (C7) to 909 km (C12) while drainage densities vary from 2.1 km/km<sup>2</sup> (C2) to 3.5 km/km<sup>2</sup> (C5) (Table 1).

When presenting the results, a distinction is made between the head catchments (Figure 2a; catchments 1–8), the intermediate subcatchments (Figure 2b catchments 9–11), and the entire study zone (Figure 2c, catchment 12).

A two-step methodology is used in this work. First the morphometric properties are analysed and then they are used to calculate GIUHs.

### 3 | MORPHOMETRIC PROPERTIES AND SCALING LAWS OF THE GREATER PARIS CSS

#### 3.1 | Methodology

Three categories of morphometric descriptors are calculated. The first are the well-known Horton-Strahler laws (law of stream numbers, stream lengths and stream areas), considered as a reference, because they have been largely used since the fifties on the basis of the

**TABLE 1** Geometrical properties of the Greater Paris combined sewer system catchments (the area  $S_0$ , the total length of the channel network  $L$ , and the drainage density  $L/S_0$ ).

Catchment	$S_0$ (km <sup>2</sup> )	$L$ (m)	$L/S_0$ (1/km)
C1	11.4	28 220	2.5
C2	65.1	133 650	2.1
C3	30.7	86 685	2.8
C4	24.3	73 515	3.0
C5	32.4	112 040	3.5
C6	8.9	30 155	3.4
C7	7.6	23 250	3.1
C8	13.4	38 950	2.9
C9	78.8	188 380	2.4
C10	141.1	412 030	2.9
C11	53.6	149 430	2.8
C12	310.0	909 150	2.9

analysis of blue lines on maps (Dodds & Rothman, 2000; Kim, 2022; Moussa & Bocquillon, 1996; Smart, 1969). The second ones are the power law properties of the exceedance probability distribution of cumulative drainage area of Rodríguez-Iturbe, Ijjasz-Vasquez, et al. (1992). They can be easily calculated from DEMs and are largely used on natural catchments (Bunster et al., 2019; Martinez et al., 2010; Rodríguez-Iturbe & Rinaldo, 1997). The third category of descriptors aims to overcome some limitations of the Horton-Strahler descriptors. Indeed, the delineation of a channel as a blue line on a topographic map is an incomplete picture of the occurrence of channels on the ground and the data on the number and length derived from the Horton-Strahler ordering system is sensitive to the inclusion or omission of ephemeral tributaries. Thus, the addition or omission of a minor channel can materially change the order designation of downstream segments. To overcome these limitations, Moussa and Bocquillon (1996) and Moussa (2003, 2009) put forward new descriptors on the basis of the relationship between a drained area threshold and morphometric properties such as the corresponding number of sources, the total channel length, and the mainstream length.

#### 3.1.1 | Horton-Strahler laws

The quantitative expressions of Horton-Strahler's laws are summarized below:

$$1. \text{ Law of stream numbers } \frac{N_{w-1}}{N_w} = R_B \quad (1)$$

$$2. \text{ Law of stream lengths } \frac{L_{w-1}}{L_w} = \frac{1}{R_L} \quad (2)$$

$$3. \text{ Law of stream areas } \frac{A_{w-1}}{A_w} = \frac{1}{R_A} \quad (3)$$

where  $N_w$  is the number of streams of order  $w$ ,  $L_w$  is the mean length of streams of order  $w$ , and  $A_w$  is the mean area contributing to streams of order  $w$  and its tributary ( $1 \leq w \leq \Omega$ ).  $R_B$  is the bifurcation ratio,  $R_L$  is the length ratio,  $R_A$  is the areas ratio and  $\Omega$  the magnitude. The values of the parameters  $R_B$ ,  $R_L$  and  $R_A$  are generally determined by plotting,  $N_w$ ,  $L_w$  and  $A_w$  versus  $w$  on semi-log diagrams and determining the 'best fit' straight lines by least squares analysis. Horton-Strahler's ratios of stream ordering ( $R_B$ ,  $R_L$  and  $R_A$ ) are often used as indicators of hydrological similarity for catchment comparison and regionalization under the assumption that if catchment attributes are identical, one would expect the surface hydrologic response to be similar. Horton-Strahler's laws were extensively used in geomorphological applications to compare and classify river systems.

#### 3.1.2 | Rodríguez-Iturbe et al.'s law

Rodríguez-Iturbe, Ijjasz-Vasquez, et al. (1992), Rodríguez-Iturbe, Rinaldo, et al. (1992) have shown that the exceedance probability distribution of cumulative drainage area is a power law form such as

$$P[A \geq a] \propto a^{-\beta} \quad (4)$$

where  $P[A \geq a] \propto a^{-\beta}$  is the probability that the contributing drainage area  $A$  be higher or equal to a given area  $a$ , and  $\beta$  an exponent. It is important to notice that often the exponent  $\beta$  is statistically indistinguishable among different catchments, and is approximately equal to  $0.43 \pm 0.04$  for OCNs while these scaling laws have begun to be studied for certain properties of urban networks such as the number of nodes and edges. Hence comparing the values of the coefficients of natural networks and urban networks is not a straightforward task.

### 3.1.3 | Moussa-Bocquillon laws

Moussa and Bocquillon (1993) suggested new power laws to characterize the main channel and their main confluence tributary connections. The method consists in using different values of a threshold area  $S$ , and for each value of  $S$ , to derive the skeleton of the network which drains at least this threshold. For each value of  $S$ , let  $N(S)$  be the total number of extremities and  $T(S)$  the total length of the channel network (Moussa, 2003). Three power laws are established:

First, a simple empirical relation  $N(S)$  is defined.

$$N(S) = \lambda \left( \frac{S}{S_0} \right)^{-\alpha} \quad (5)$$

where  $S_0$  is the catchment area, and  $\alpha$  and  $\lambda$  are two parameters to be adjusted. Moussa (2009) shows that the value of parameter  $\alpha$  is close to 1.

The second law expresses the total length of the channel network  $T(S)$ :

$$T(S) = (m_1 + bS_0^{0.5}) \left( \frac{S}{S_1} \right)^{-\alpha+0.5} - bS_0^{0.5} \quad (6)$$

where  $b$  is a parameter to be adjusted;  $m_1$  is a characteristic distance and  $S_1$  a characteristic area which can be calculated from a DEM (see details in Moussa, 2003).

The third law is a simplification of Equation (5) under the assumption that  $\alpha = 1$ , we define

$$U = \frac{NS}{S_0} \quad (7)$$

which tends to be a constant whose value varies between 0.22 and 0.3 for low values of  $S/S_0$  for OCNs while this property is not verified for non-OCNs (Moussa et al., 2011).

In practice, the parameter  $\beta$  in Equation (4), the parameters  $\alpha$  and  $\lambda$  in Equation (5), the parameter  $b$  in Equation (6), and the constant  $U$  in Equation (7) are adjusted by minimizing the RMSE error between the observed points and the adjusted laws on the linear part of the curves corresponding to low values of  $S/S_0$ .

### 3.1.4 | Comparison criteria

The comparison between the observed points and the adjusted laws is based on the following criteria:

- the coefficient of determination ( $\rho$ ) when straight lines are adjusted; this is the case for the three Horton-Strahler laws ( $R_B$ ,  $R_L$  and  $R_A$ ), the power law of Rodríguez-Iturbe, Ijjasz-Vasquez, et al. (1992), and the N(S) power law of Moussa-Bocquillon. For Horton-Strahler laws, Moussa (2008, 2009) presents a detailed discussion on the regression method for both the Horton-Strahler laws and the new equivalent laws proposed by Moussa (2009). For the Rodríguez-Iturbe and Moussa-Bocquillon laws, one of the main difficulties is to define the interval of  $S/S_0$  for which the adjustment has to be carried out. Moussa et al. (2011) presented a detailed method for the classification of the internal nodes of the channel network which allows to determine the limits of the interval of  $S/S_0$  on which the adjustment is carried out.
- the Nash-Sutcliffe Efficiency (NSE) criterion when comparing two curves; this is the case of the  $T(S)$  law of Moussa-Bocquillon. For non-linear regressions, the best-fit curve is often assumed to be that which minimizes the sum of the ordinary least squares (OLS). This criterion gives similar results to the well-known NSE because there is a simple linear relationship between NSE and OLS with  $NSE = 1 - (OLS/Constant)$ .
- the coefficient of variation ( $c_v$ ) when dealing with the constant  $U$  of Moussa-Bocquillon.

Table 2 shows the definitions we use in this section for the terms 'Very good', 'Good' or 'Fair' when discussing the three criteria  $\rho$ , NSE and  $c_v$ .

### 3.1.5 | Applying the scaling laws to combined sewer systems (CSS)

The question that arises is whether the scaling laws established for OCNs may also be true for non-OCN urban CSSs. To answer this question, each CSS is characterized by the three categories of morphometric descriptors:

- Horton-Strahler laws: first we check if the laws of stream numbers, lengths and areas are verified by calculating the determination coefficient of the regression, and then we compare the ranges of the parameters  $R_B$ ,  $R_L$  and  $R_A$  obtained on CSSs to those reported in the literature for natural catchments:  $3 < R_B < 5$ ,  $1.5 < R_L < 3.5$  and  $3 < R_A < 6$  (Rodríguez-Iturbe & Rinaldo, 1997; Smart, 1969).
- Rodríguez-Iturbe et al.'s power law: first we check if the scaling law is verified by calculating the determination coefficient of the regression, and then we compare the value of the exponent  $\beta$  to the range obtained for natural OCNs:  $0.39 < \beta < 0.47$  (Rodríguez-Iturbe et al., 2011).

- Moussa-Bocquillon laws: first we check if the two power laws  $N(S)$  and  $T(S)$  are verified by calculating the determination coefficient of the regression, and then we compare the values of parameters  $\alpha$ ,  $\lambda$ ,  $U$  and  $b$  to those obtained by Moussa (1997, 2003, 2008, 2009), Moussa et al. (2011) and Bamufleh et al. (2020) on natural catchments:  $0.78 < \alpha < 1.29$ ,  $0.17 < \lambda < 0.47$ ,  $0.23 < U < 0.32$  and  $-3.96 < b < 2.38$ .

### 3.2 | Results

Applications were carried out on the twelve catchments C1 to C12. In this section we present in detail the results of the morphometric analysis for the two catchments C3 and C4. These two catchments have been chosen as they have very similar area ( $S_0$ ) and drainage density

( $L/S_0$ ) and different channel network shapes. The Data S1 show the results for all catchments.

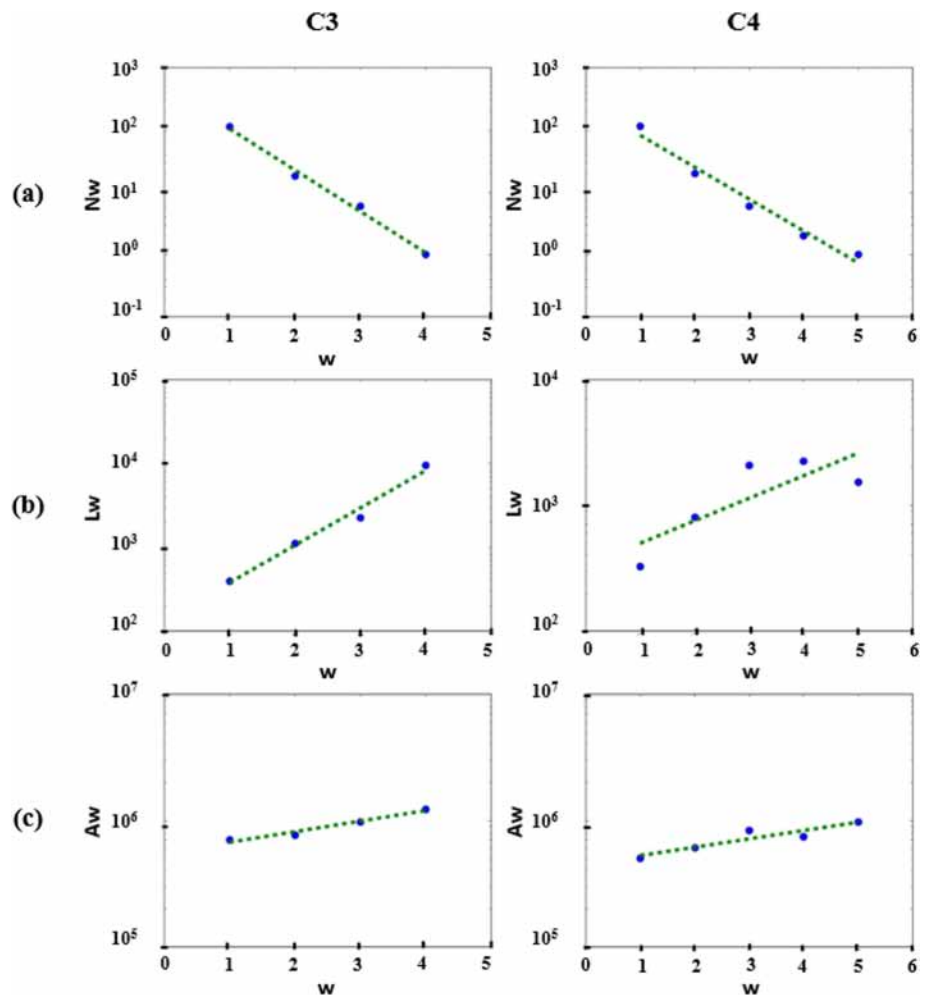
#### 3.2.1 | Horton-Strahler laws

Figure 3 shows the graphs obtained for the three Horton-Strahler laws, in a log scale, for catchments C3 and C4. For C3, the linear regression using 4 points is well verified indicating that the laws are respected in this case. However, for C4, the linear regression using 5 points is not respected for the law of stream lengths but applicable for the laws of stream areas and stream numbers.

Table 3 presents the results of the Horton-Strahler ratios for the studied networks. According to the literature, the values of  $R_B$ ,  $R_L$  and

**TABLE 2** Definition of performance levels.

Criteria	Very good (***)	Good (**)	Fair (*)
Determination coefficient $\rho$	$\rho > 0.95$	$0.9 < \rho < 0.95$	$\rho < 0.90$
Nash-Sutcliffe efficiency NSE	$NSE > 0.95$	$0.9 < NSE < 0.95$	$NSE < 0.90$
Coefficient of variation $c_v$	$c_v < 0.3$	$0.3 < c_v < 0.5$	$c_v > 0.5$



**FIGURE 3** Horton-Strahler laws: Law of stream numbers (a), law of stream lengths (b), and law of stream areas (c), blue points correspond to the catchment values and the dotted green line to the fitted line for catchments C3 and C4.

**TABLE 3** Horton–Strahler characteristics ( $\Omega$  and  $L_{\Omega}$ ) and ratios ( $R_B$ ,  $R_L$ ,  $R_A$ , from Equations 1, 2 and 3) for the 12 Greater Paris CSS catchments.

Catchment	$\Omega$	$L_{\Omega}$ (in m)	$R_B$ and ( $\rho$ )	$R_L$ and ( $\rho$ )	$R_A$ and ( $\rho$ )
C1	4	722	3.0 (***)	1.3 (*)	1.2 (*)
C2	5	8060	3.3 (***)	1.9 (***)	1.5 (**)
C3	4	9466	4.6 (***)	2.8 (***)	1.2 (***)
C4	5	1524	3.3 (***)	1.5 (*)	1.2 (*)
C5	5	4066	3.5 (***)	1.8 (**)	1.2 (***)
C6	4	3294	3.6 (***)	2.1 (***)	1.2 (***)
C7	4	555	3.3 (***)	1.3 (*)	1.1 (*)
C8	4	3694	3.6 (***)	2.2 (**)	1.1 (*)
C9	5	21 167	3.5 (***)	2.3 (**)	1.2 (*)
C10	6	14 098	3.6 (***)	1.8 (*)	1.2 (*)
C11	5	22 085	3.7 (***)	2.3 (**)	1.2 (*)
C12	6	14 098	3.9 (***)	2.1 (***)	1.1 (**)

Note: The criteria level of  $\rho$  (Table 2) are shown in parentheses. The exact values of  $\rho$  are provided in the Data S1 (S9). \*\*\* Very good performance. \*\* Good performance. \* Fair performance.

$R_A$  are generally in the range [3; 5], [1.5; 3.5] and [3; 6] respectively for natural networks (Rodríguez-Iturbe & Rinaldo, 1997; Smart, 1969). In the case of the 12 catchments of the Greater Paris CSS, the magnitude  $\Omega$  ranges between 4 and 6. The law of stream numbers is always verified such that the bifurcation ratio  $R_B$  is between 3 and 4.6 with a coefficient of determination greater than 0.95. Whereas for the law of stream lengths, in 4 out of 12 cases (C1, C4, C7 and C10), the corresponding regression is not verified and yields a determination coefficient lower than 0.9. But when the law is verified (with a determination coefficient higher than 0.9), the value of the length ratio  $R_L$  is in the same interval as that corresponding to the natural networks. The law of areas is not verified for 7 out of 12 cases (C1, C4, C7, C8, C9, C10, and C11) and yields a determination coefficient lower than 0.9. Moreover, the area ratio  $R_A$  is never in the interval [3; 6] corresponding to the natural networks.

The reason for which Horton–Strahler's law is not verified for anthropogenic networks can be explained by the fact that the formation of natural networks follows the law of erosion and networks reach equilibrium under the effect of gravity whereas for CSSs, the design criterion is ruled by the optimization between pipe and excavation price. In addition, the connection angles in the natural case are always smooth (Seybold et al., 2017), while perpendicular connections occur in CSSs. Moreover, new housing estates that are built after a sanitation plan has been implemented may modify the original design rules which generally favour gravity fed flow: although CSSs were not implemented after the 60s, new WWTPs were added and the outlets were modified. This may affect parameter  $R_L$  that describes the ratio between the lengths of different stream orders. Indeed, when comparing the shape of natural networks to that of CSSs, we find a difference in the tree structure and in the distance between the various branches corresponding to the “streams”. Thus, the area drained by

each branch does not necessarily correspond to what a natural stream may drain.

### 3.2.2 | Rodríguez-Iturbe power law

Figure 4 shows in a log–log scale graphs of the power-law distribution of the upstream contributing area for catchments C3 and C4. A line is well fitted on the linear part of the graph. Table 4 presents the value of the slope  $\beta$  of the fitted line corresponding to the Rodríguez-Iturbe power law (Equation 4). This law is always verified in the case of the twelve catchments of the Greater Paris CSS such that the value of  $\beta$  is between 0.4 and 0.53 with a coefficient of determination greater than 0.95. For natural catchments and OCNs this slope has a value of 0.43  $\pm$  0.04 (Rodríguez-Iturbe et al., 2011).

### 3.2.3 | Moussa-Bocquillon laws

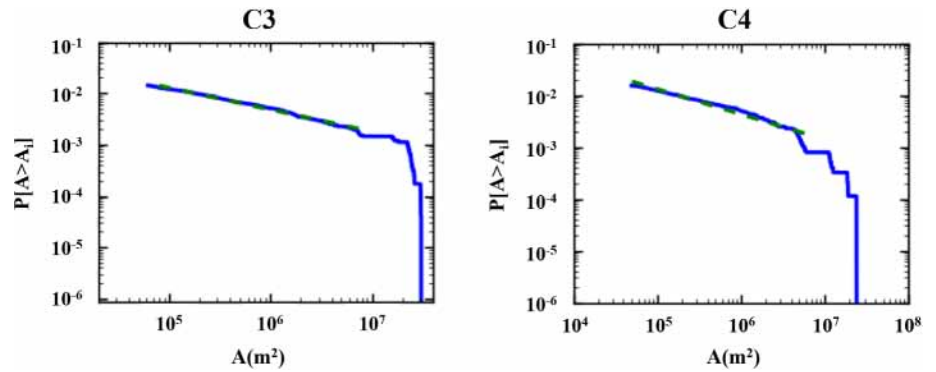
Figure 5 shows the results of three Moussa-Bocquillon laws for catchments C3 and C4: N(S) from Equation (5), T(S) from Equation (6) and the constant U from Equation (7). For C3, the regression line is very well fitted for the relation between N and T as function of  $S/S_0$  but concerning the relation of U as function of  $S/S_0$ , the green line corresponding to U does not fit the totality of the curve. This means that the third law of Moussa-Bocquillon is not verified for C3 (Figure 5a,b). The same result is observed for C4 with a lower correlation for the relation between T and  $S/S_0$  (Figure 5c).

Table 5 presents the results of the Moussa-Bocquillon morphometric descriptors. The values of  $\alpha$  and  $\lambda$  are obtained through a regression between N and  $S/S_0$  Equation (5). A determination coefficient higher than 0.95 is calculated for all twelve catchments of the Greater Paris CSS. This relation is always verified with a value of  $\alpha$  between 0.83 and 0.99 while for natural networks it ranges between 0.78 and 1 (Bamufleh et al., 2020; Moussa, 1997, 2003, 2008, 2009). Moreover, the value of  $\lambda$  is between 0.3 and 0.6 while for natural catchments it is between 0.15 and 0.5 (Bamufleh et al., 2020; Moussa, 2008, 2009). Furthermore, the value of b, which is the result of the relation between T and  $S/S_0$ , ranges between 0.3 and 4.3 for the twelve catchments of the Greater Paris CSS, while for natural catchments it ranges between  $-4$  and 2.5 (Bamufleh et al., 2020; Moussa, 2008, 2009).

In the case of natural catchments, and according to 10 examples from the literature (Bamufleh et al., 2020; Moussa, 2009), the value of  $R_{Be}$ ,  $R_{Le}$  and  $R_{Ae}$  are in the range [4.5; 8.5], [4; 8.5] and [2; 3] respectively. In the case of the twelve catchments of the Greater Paris CSS, the two laws corresponding to the geomorphological relations are always verified with a coefficient of determination higher than 0.95. However, the values of  $R_{Be}$ ,  $R_{Le}$  and  $R_{Ae}$  are in the range [3.9; 6.6], [3; 6.5] and [2; 2.5] respectively. Although this difference in range may be due to the limited number of natural catchments (only 10) for which these ratios are available in the literature, the verification of the geomorphic relationships is true and indicates that the Horton



**FIGURE 4** Rodriguez-Iturbe law: the power-law distribution of the upstream contributing area for catchments C3 and C4 (blue line calculated from generated network, green dotted line is adjusted on the linear part of the curve).



**TABLE 4** Rodriguez-Iturbe power law  $\beta$  (from Equation (4)) for the 12 Greater Paris CSS catchments.

Catchment	$\beta$ and ( $p$ )
C1	0.40 (***)
C2	0.48 (***)
C3	0.43 (***)
C4	0.49 (***)
C5	0.47 (***)
C6	0.48 (***)
C7	0.53 (***)
C8	0.48 (***)
C9	0.45 (***)
C10	0.51 (***)
C11	0.44 (***)
C12	0.51 (***)

Note: The criteria level of  $p$  (Table 2) are shown in parentheses. The exact values of  $p$  are provided in the Data S1 (S9). \*\*\* Very good performance. \*\* Good performance. \* Fair performance.

Strahler equivalent parameters obtained through these relationships can still be used to calculate a geomorphic unit hydrograph for CSSs. The parameters ( $a$ ,  $b$ ) of the Nash unit Hydrograph ( $G_N$ ) were related to Horton order ratios by Rosso (1984) on the basis of observations of natural catchments. He obtained the two expressions of Equation (9). As it is not possible to adapt these expressions to CSSs, one must assume that they remain valid in this context. This assumption applies also to the Nash unit hydrograph equivalent ( $G_{Ne}$ ).

## 4 | A HYDROLOGICAL USE CASE: THE GIUHS OF THE GREATER PARIS CSS

### 4.1 | Methodology

Unit Hydrograph is a widely used method to represent the response of a catchment to rainfall impulse when runoff is a dominant process which is the case in urban areas. The derivation of the unit hydrograph from the geomorphological features of the catchment gave rise

to the concept of Geomorphological Instantaneous Unit Hydrograph (hereafter GIUH), detailed in the text book by Rodriguez-Iturbe and Rinaldo (1997). Several approaches have been proposed to derive the GIUH of a catchment, among which four are compared in this section using the descriptors calculated in the previous section: a simplified version of the Width Function based GIUH (noted  $G_{WFF}$ ) (Rodríguez-Iturbe & Rinaldo, 1997), the classical Nash (1957) unit hydrograph (noted  $G_N$ ) of which the two parameters are estimated from the Horton-Strahler descriptors (Rosso, 1984), the modified GIUH (noted  $G_{Ne}$ ) which is an adaptation of the previous GIUH to the new Moussa-Bocquillon descriptors (Moussa, 2009), and a unit hydrograph solution of the Diffusive Wave Equation on the basis of the Hayami (1951) equation (noted  $G_H$ ) with physical parameters.

#### 4.1.1 | Width function based GIUH ( $G_{WFF}$ )

The width function  $G_{WFF}$  is defined as the Probability Density Function (PDF) of the hydrologic distance to the catchment outlet (Kirkby, 1976). Rinaldo et al. (1992) proposed to model the travel time along hydrologic paths by an inverse Gaussian PDF defined by two parameters: velocity and coefficient of dispersion. The convolution of the two PDFs leads to the expression of the width function based GIUH (see Rigon et al., 2016 for a recent review). In the present work, it is assumed that the dispersion of flow along hydrologic paths can be neglected which allows to directly deduce the GIUH from the width function by a simple change of unit of distance into time involving the flow velocity  $v$ .

#### 4.1.2 | Nash unit hydrograph ( $G_N$ )

Rosso (1984) showed that the shape of the founding GIUH formulation (Rodríguez-Iturbe & Valdés, 1979) was correctly preserved by the Nash unit hydrograph (Nash, 1957) by expressing the two parameters ( $a$ ,  $k$ ) of the Nash model as a function of Horton-Strahler ratios:  $R_B$ ,  $R_L$ ,  $R_A$ , and  $L$  length of highest-order stream,

$$G_N(a, k, t) = \left(\frac{t}{k}\right)^{a-1} \frac{e^{-t/k}}{k\Gamma(a)} \quad (8)$$

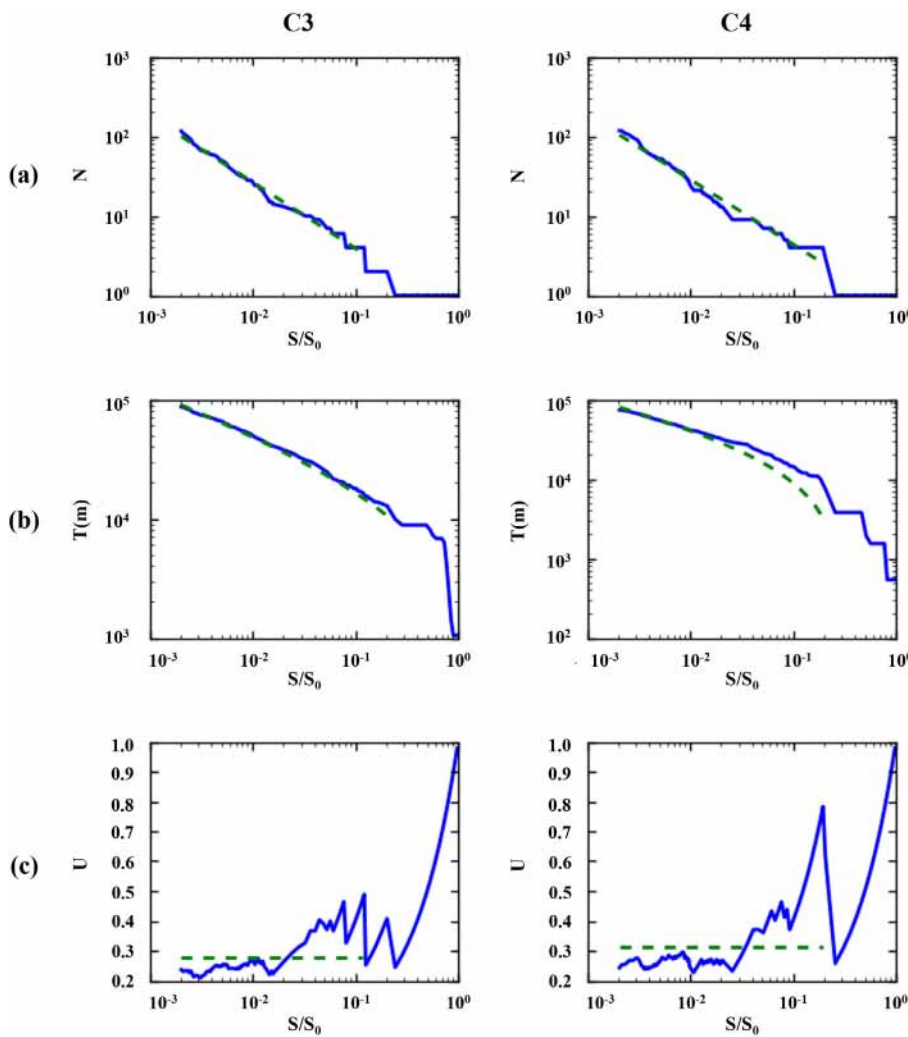


**FIGURE 5** Moussa-Bocquillon laws function of the threshold area  $S/S_0$  for catchments C3 and C4 (blue line calculated from generated network, green dotted line is adjusted on the linear part of the curve): (a) the total number of source nodes  $N$ ; (b) the total length of the channel network  $T$ ; (c) the term  $U = N \cdot S/S_0$ .

Catchment	N(S)			T(S)		U			$G_{Ne}$		
	$\alpha$	$\lambda$	$\rho$	b	NSE	$\mu$	$\sigma$	$c_v$	$R_{Ae}$	$R_{Be}$	$R_{Le}$
C1	0.89	0.4	***	2.3	*	0.26	0.138	*	5.6	4.6	2.4
C2	0.99	0.3	***	0.7	***	0.36	0.164	**	6.4	6.5	2.6
C3	0.83	0.6	***	2.1	***	0.28	0.160	*	3.9	3.1	2.0
C4	0.86	0.5	***	4.3	***	0.31	0.168	*	4.9	4.0	2.2
C5	0.89	0.5	***	3.3	***	0.28	0.157	*	4.8	4.0	2.2
C6	0.98	0.3	***	2.6	***	0.29	0.113	**	6.6	6.4	2.6
C7	0.86	0.5	***	3.3	***	0.28	0.182	*	4.9	4.0	2.2
C8	0.86	0.4	***	2.8	**	0.25	0.167	*	5.3	4.2	2.3
C9	0.94	0.4	***	0.3	***	0.31	0.148	**	5.0	4.6	2.2
C10	0.89	0.5	***	2.3	***	0.30	0.184	*	4.2	3.6	2.0
C11	0.86	0.5	***	1.6	***	0.27	0.137	*	4.1	3.4	2.0
C12	0.91	0.5	***	2.8	***	0.30	0.145	**	4.4	3.8	2.1

Note: The corresponding criteria levels of  $\rho$ , NSE and  $c_v$  (Table 2) are shown. The exact values of  $\rho$ , NSE and  $c_v$  are provided in the Data S1 (S9). \*\*\* Very good performance. \*\* Good performance. \* Fair performance.

**TABLE 5** Moussa-Bocquillon descriptors for the 12 Greater Paris CSS catchments: (i)  $N(S)$ : the parameters  $\alpha$  and  $\lambda$  and the coefficient of determination  $\rho$  of the adjusted law; (ii)  $T(S)$ : the parameter  $b$ , and the Nash-Sutcliffe Efficiency NSE of the adjusted law; (iii)  $U$ : the mean value  $\mu$ , the standard deviation  $\sigma$  and the variation coefficient  $c_v = \sigma/\mu$ ; (iv) the parameters  $R_{Ae}$ ,  $R_{Be}$  and  $R_{Le}$  of the  $G_{Ne}$ .

$$\text{with } a = 3.29 \left( \frac{R_B}{R_A} \right)^{0.78} R_L^{0.07} \text{ and } k = 0.7 \left( \frac{R_A}{R_B R_L} \right)^{0.48} \frac{L}{v} \quad (9)$$

where  $v$  is the flow velocity, and  $\Gamma$  is the gamma function.

#### 4.1.3 | Nash unit hydrograph equivalent ( $G_{Ne}$ )

In order to overcome the limitations of the Horton-Strahler classification, Moussa (2003, 2009) put forward new descriptors to characterize morphometric properties of the channel network, classify the internal nodes of the channel network, and establish the relationship between the shape of the network and the hydrological response.

$$\begin{aligned} R_{Be} &= \frac{2^\alpha}{\lambda}, R_{Ae} = \left( \frac{2^\alpha}{\lambda} \right)^{\frac{1}{\alpha}}, R_{Le} = \left( \frac{2^\alpha}{\lambda} \right)^{\frac{1}{2\alpha}} \text{ and} \\ L_e &= \left( m_1 + bS_0^{0.5} \right) \left( \frac{S_1}{2S_0} \right)^{\alpha-0.5} \frac{R_{Be} - R_{Le}}{R_{Le}} \end{aligned} \quad (10)$$

The four new descriptors ( $R_{Be}$ ,  $R_{Le}$ ,  $R_{Ae}$  and  $L_e$ ) replace those of the Horton-Strahler laws ( $R_B$ ,  $R_L$ ,  $R_A$  and  $L_e$ ) in the Nash unit hydrograph introduced in the previous paragraph, Equations (8) and (9), and a new expression of the parameters ( $a$ ,  $k$ ) is obtained.

#### 4.1.4 | Hayami function ( $G_H$ )

Moussa (1997) proposed a formulation of the GIUH based on the Hayami (1951) approximation solution of the diffusive wave equation especially adapted for the routing hydrograph through a channel network. The  $G_H$  is expressed:

$$G_H(C, D, t) = \frac{\bar{L}}{2(\pi D)^{0.5}} \frac{e^{-\frac{1.67\bar{L}}{4D} \left( 2 - \frac{\bar{L}}{1.67\bar{v}t} - \frac{1.67\bar{v}t}{\bar{L}} \right)}}{t^{1.5}} \quad (11)$$

where  $t$  is time,  $\bar{L}$  is the mean flow path length to the outlet,  $v$  ( $\text{m s}^{-1}$ ) the velocity and  $D$  ( $\text{m}^2 \text{s}^{-1}$ ) the coefficient of dispersion (Chow et al., 1988). In the applications  $D$  was considered equal to the geomorphologic dispersion as suggested by Rinaldo et al. (1992), Saco and Kumar (2002a), (2002b), Rossel et al. (2014), and Jovanovic et al. (2019):

$$D = \frac{1}{2} \text{var}(L) \times \langle T \rangle^{-1} \quad (12)$$

where  $\text{var}(L)$  represents the variance of all network flowpath lengths, and  $\bar{T}$  the mean travel time of all flowpaths in the network.  $D$  assumes uniform velocity across the network where  $v = \bar{L}/\bar{T}$ .

#### 4.1.5 | Characterizing the GIUHs of the Greater Paris CSS

The question is how the morphometric descriptors of non-OCN CSSs may impact the shape of the GIUH. For this, each CSS network is

characterized by the expressions of GIUHs. Each of the four GIUHs has a parameter that expresses the velocity  $v$  which needs to be calibrated when rainfall/runoff data are available. In this application, the objective is to compare the four GIUHs for the same value of  $v$ , herein considered  $v = 1 \text{ m.s}^{-1}$  as it is a plausible value (Jovanovic et al., 2019).

On each CSS network, each of the four GIUHs is characterized by three variables: the maximum value of the GIUH  $g_p$  and its time of occurrence  $T_p$ , and its center of gravity  $T_G$  (sometimes denoted lag time). The three variables ( $T_p$ ,  $g_p$ ,  $T_G$ ) are useful: (i) to compare the four GIUHs for a given CSS network; (ii) for a given GIUH type, to compare and classify networks according to each criterion.

The GIUH comparison is based on the coefficient of variation  $c_v$  when comparing the characteristics ( $T_p$ ,  $g_p$  and  $T_G$ ) of the four GIUHs ( $G_{WF}$ ,  $G_N$ ,  $G_{Ne}$  and  $G_H$ ).

## 4.2 | Results

Figure 6 shows a comparison between the four GIUHs, for the twelve catchments C1 to C12. The graphs show similar results between the  $G_{WF}$  and the  $G_H$  for the 12 catchments. While for the  $G_N$ , when one of the three Horton-Strahler laws is not verified (with a coefficient of determination lower than 0.9 as for catchments C1, C4, C7, C8, C9, C10 and C11), the hydrograph corresponding to the GIUH produces a response that is deviated from that of the other three functions ( $G_{Ne}$ ,  $G_H$  and  $G_{WF}$ ). Note that in the 5 cases where all adjusted laws yield “very good” performance criteria as defined in Table 2, the  $G_N$  is sometimes closer to the response given by the  $G_H$  and the  $G_{WF}$  (C5) and sometimes closer to those of the  $G_{Ne}$  (C2, C3, C6, C12). Concerning the  $G_{Ne}$ , by comparing it with the two other functions, the  $G_{WF}$  and the  $G_H$ , we notice that maximum value of the GIUH ( $g_p$ ) corresponds to half the value of the 2 other functions while the time of occurrence of  $g_p$  is approximately the same in the 12 cases.

Table 6 shows the values of the time of occurrence of  $g_p$  ( $T_p$ ), the maximum value of the GIUH ( $g_p$ ) and the time of occurrence of the centre of gravity ( $T_G$ ) of each hydrograph. In terms of peak time, the value obtained through the  $G_{Ne}$ 's is identical to that of  $G_H$  for 5 cases out of 12, and for 3 out of 12 cases it is closer to that of the  $G_{WF}$ . This shows a similarity between the response obtained by the  $G_{Ne}$  (calculated through morphometric parameters) and the other two functions calculated through average values of distance and time in the case of  $G_H$ , and distances to the outlet in the case of the  $G_{WF}$ . When comparing the  $G_H$  and the  $G_{WF}$ , the ratio of  $g_p$  values of these 2 functions vary between 0.8 and 1 for 12 cases, and the ratio of  $T_p$  values vary between 1 and 1.3 in 9 cases, and between 1.3 and 2 in 3 cases. When comparing the coordinates corresponding to the centre of gravity of the hydrographs of these 2 functions, the ratio of the GIUH value varies between 0.8 and 1.3 and the ratio of time varies between 0.8 and 1 in all cases. This shows high similarity between these 2 functions in terms of computed hydrological response.

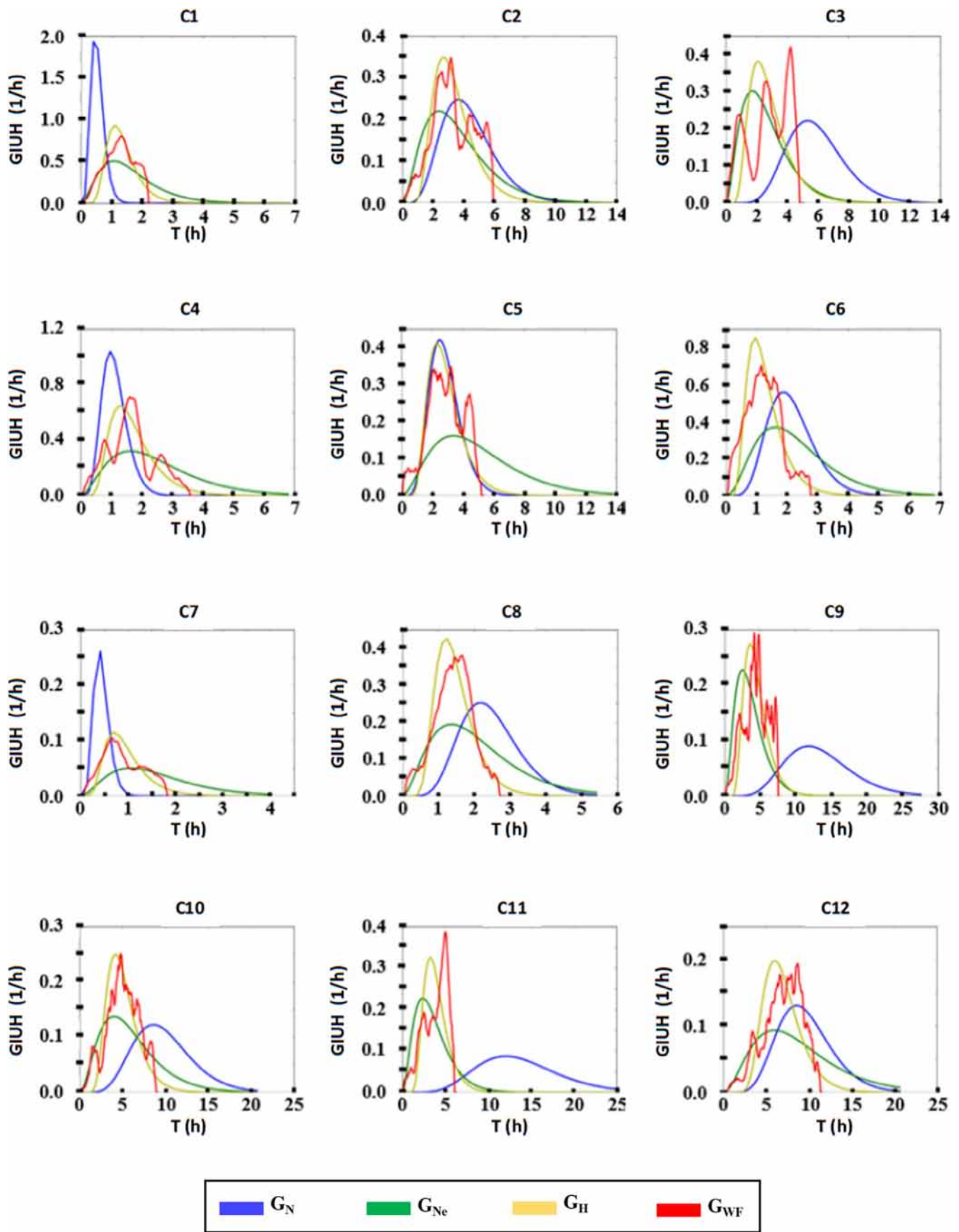


FIGURE 6 Comparison between four GIUHs ( $G_{WF}$ ,  $G_N$ ,  $G_{Ne}$  and  $G_H$ ) for the twelve catchments of the Greater Paris CSS.

**TABLE 6** Characteristics of the four GIUHs ( $G_{WF}$ ,  $G_N$ ,  $G_{Ne}$  and  $G_H$ ) for the 12 Greater Paris CSS catchments: time of occurrence of the peakflow ( $T_p$ ), peakflow ( $g_p$ ) and time of occurrence of the centre of gravity ( $T_G$ ).

Catchment	$T_p$ (h)				$g_p$ (1/h)				$T_G$ (h)			
	$G_N$	$G_{Ne}$	$G_H$	$G_{WF}$	$G_N$	$G_{Ne}$	$G_H$	$G_{WF}$	$G_N$	$G_{Ne}$	$G_H$	$G_{WF}$
C1	0.4	1.1	1.1	1.3	1.9	0.5	0.9	0.8	0.6	1.9	1.6	1.2
C2	3.6	2.4	2.6	3.2	0.3	0.2	0.4	0.4	4.4	3.6	3.6	3.3
C3	5.3	1.7	2.1	4.3	0.2	0.3	0.4	0.4	6	2.8	3.1	2.5
C4	1	1.7	1.3	1.6	1.0	0.3	0.6	0.7	1.3	2.6	2.0	1.8
C5	2.5	3.3	2.4	3.2	0.4	0.2	0.4	0.4	3	4.7	3.1	2.6
C6	1.9	1.7	1.0	1.2	0.6	0.4	0.9	0.7	2.3	2.5	1.5	1.4
C7	0.4	1.1	0.7	0.7	2.6	0.5	1.2	1.1	0.5	1.9	1.2	1.0
C8	2.2	1.4	1.3	1.7	0.5	0.4	0.9	0.8	2.6	2.3	1.7	1.4
C9	11.8	2.5	3.6	4.2	0.1	0.2	0.3	0.3	12.5	3.7	4.6	4.4
C10	8.6	4.0	4.2	4.8	0.1	0.1	0.3	0.3	9.3	5.3	5.1	5.1
C11	12.1	2.4	3.2	5.0	0.1	0.2	0.3	0.4	12.8	3.5	4.1	3.6
C12	8.6	6.0	6.0	8.7	0.1	0.1	0.2	0.2	9.3	7.2	6.9	6.8

**TABLE 7** For each catchment, arithmetic mean ( $\mu$ ), sample standard deviation ( $\sigma$ ) and coefficient of variation ( $c_v$ ) of the four GIUHs ( $G_{WF}$ ,  $G_N$ ,  $G_{Ne}$  and  $G_H$ ) in Table 5.

Catchment	$T_p$ (h)			$g_p$ (1/h)			$T_G$ (h)		
	$\mu$	$\sigma$	$c_v$	$\mu$	$\sigma$	$c_v$	$\mu$	$\sigma$	$c_v$
C1	0.98	0.39	**	1.03	0.61	*	1.33	0.56	**
C2	2.95	0.55	***	0.33	0.10	***	3.50	0.47	***
C3	3.35	1.73	*	0.37	0.10	***	2.80	1.62	*
C4	1.40	0.32	***	0.53	0.29	*	2.13	0.54	***
C5	2.85	0.47	***	0.33	0.10	***	3.47	0.93	***
C6	1.45	0.42	***	0.67	0.21	**	1.80	0.56	**
C7	0.73	0.29	**	0.93	0.89	*	1.37	0.58	**
C8	1.65	0.40	***	0.70	0.24	**	1.80	0.55	***
C9	5.53	4.24	*	0.27	0.10	**	4.23	4.15	*
C10	5.40	2.16	**	0.23	0.12	**	5.17	2.07	**
C11	5.68	4.42	*	0.30	0.13	**	3.73	4.54	*
C12	7.33	1.53	***	0.17	0.06	**	6.97	1.18	***

Note: The corresponding criteria levels of  $c_v$  (Table 2) are shown. The exact values of  $c_v$  are provided in the Data S1 (S9). \*\*\* Very good performance. \*\* Good performance. \* Fair performance.

In order to compare the four GIUHs, Table 7 shows the arithmetic mean, the sample standard deviation, and the coefficient of variation for each catchment and for each of the three variables ( $T_p$ ,  $g_p$ , and  $T_G$ ). We observe that for the catchments C2, C5, C8 and C12 we have low values of  $c_v$  for the three variables with  $0.13 < c_v < 0.34$ . This reflects that the four GIUHs are comparable and have the same characteristics. This result reflects also that the different scaling laws are verified and give comparable results. On the other hand, catchments C1, C7, C10 and C11 have high  $c_v$  values for all three variables with  $0.40 < c_v < 1.22$ . This is due to large differences in the shapes of the GIUHs which may be due to either non-verification of the power laws or high variability of the descriptors.

One may question if the scaling laws are verified, how they may impact the shape of the GIUH? For the three catchments C2, C5 and C8, we obtain very good performances of  $c_v$  when comparing the  $T_p$ ,  $Q_p$  and  $T_G$  of the four GIUHs (12 very good). On the opposite, the four catchments C1, C7, C10 and C11 yield the lowest performances regarding  $c_v$  (8 good, 4 fair). For the cases where the power laws are verified (C3, C5, C6 and C12), the GIUHs can be calculated. Table 8 shows that for these 4 catchments the characteristics of the four GIUHs are comparable for the selected criteria as reflected by the low values of  $c_v$  for ( $T_p$ ,  $g_p$  and  $T_G$ ) and consequently higher performances (8 very good, 2 good and 2 fair). On the contrary, catchments C1, C4, C7 and C10 which show low

Catchment	Horton-Strahler			R-I	Moussa-Bocquillon			GIUH		
	$R_B$	$R_L$	$R_A$	$\beta$	N(S)	T(S)	U	$T_p$	$g_p$	$T_g$
	$\rho$	$\rho$	$\rho$	$\rho$	$\rho$	NSE	$c_v$	$c_v$	$c_v$	$c_v$
C1	***	*	*	***	**	*	*	**	*	**
C2	***	***	**	***	***	***	**	***	***	***
C3	***	***	***	***	***	***	*	*	***	*
C4	***	*	*	***	***	***	*	***	*	***
C5	***	**	***	***	***	***	*	***	***	***
C6	***	***	***	***	***	***	**	***	***	**
C7	***	*	*	***	***	***	*	**	*	**
C8	***	**	*	***	***	**	*	***	***	***
C9	***	**	*	***	***	***	**	*	***	*
C10	***	*	*	***	***	***	*	**	**	**
C11	***	**	*	***	***	***	*	*	**	*
C12	***	***	**	***	***	***	**	***	**	***

Note: The corresponding criteria levels of  $\rho$ , NSE and  $c_v$  (Table 2) are shown. The exact values of  $\rho$ , NSE and  $c_v$  are provided in the Data S1 (S9). \*\*\* Very good performance. \*\* Good performance. \* Fair performance.

performances for the power laws yield also low performances when comparing the four GIUHs with high values of  $c_v$  for ( $T_p$ ,  $g_p$  and  $T_g$ ) (2 very good, 7 good and 3 fair). Consequently, when power laws are verified, all four GIUHs give generally comparable results.

## 5 | DISCUSSION

CSSs are very specific objects whose topology depends on several factors among which: structure of the city, evolution of this city over time, topography, urban water management policy, and characteristics of the hydrographic network. The development of centralized sewer systems during the 19th century has resulted from several factors detailed by Burian et al. (2000): fast urban growth, extension of water supply networks, and most of all, crucial importance of sewage and wastewater collection to improve public health. The early networks have been expanded and modified according to urban sprawl and the constraints of urban planning (Gironás et al., 2009). At the time Paris, as most cities, had chosen to design combined sewer networks. The flow of combined water networks resulted in contamination and degradation of water bodies. The development of treatment plants for waste and combined water and the separation of wastewater from stormwater, occurred during the second part of the 20th century (Laroulandie, 1993; Reid, 1993). These factors have certainly influenced the morphometric properties of the Greater Paris CSS network. The morphometric properties might also depend on the properties of the street network (Courtat et al., 2011). While scale-free power law distributions were largely studied and verified for natural channel networks with complex topology considered as Optimal

**TABLE 8** Criteria levels for the adjusted laws: the determination coefficient  $\rho$  for the three Horton-Strahler laws ( $R_B$ ,  $R_L$  and  $R_A$ ), the Rodriguez-Iturbe (noted R-I) power law ( $\beta$ ) and Moussa-Bocquillon N(S); the Nash-Sutcliffe Efficiency NSE for Moussa-Bocquillon T(S). The coefficient of variation  $c_v$  for Moussa-Bocquillon U and the three GIUHs descriptors ( $T_p$ ,  $g_p$  and  $T_g$ )

Channel Networks (Rigon et al., 1993; Rodriguez-Iturbe & Rinaldo, 1997), and for many other large networks (i.e., genetic network or the World Wide Web; Barabási & Albert, 1999; Albert & Barabási, 2002), the study of urban drainage networks suffers from the lack of data (Masucci et al., 2014; Yang et al., 2017). It could be interesting to apply the methodology proposed by Yang et al. (2017) to the Greater Paris CSS. Indeed, the authors analysed the evolution of the urban drainage network of two cities and showed that the studied networks evolve to the state topologically similar to rivers. Unfortunately, it would represent a very important work on the history of the Greater Paris urban data, over a century and that is not feasible within this study. An alternative might be to compare the urban topology of catchments according to their period of urban development. This work aims to calculate the morphometric descriptors and the corresponding GIUHs on the Greater Paris CSS, and has a dual purpose. The first objective is to check whether the three categories of scaling laws (Horton-Strahler, Rodriguez-Iturbe and Moussa-Bocquillon) are verified or not for the Greater Paris CSS. The results show that most of these laws are verified on the majority of the twelve studied subcatchments, but for some of them, the descriptor values do not fall within the range of those of natural networks. The second objective aims to go further, by using the previously obtained descriptors to calculate the GIUHs. Of course, the main assumption is that the mathematical expressions of the GIUHs proposed in the literature for natural hydrographic networks are applicable to CSS networks. This is the case for the Nash unit hydrograph ( $G_N$ ) using Horton-Strahler ratios and the equivalent Nash unit hydrograph ( $G_{Ne}$ ) using Moussa-Bocquillon descriptors. Note that the Width Function ( $G_{WF}$ ) and the Hayami function ( $G_H$ ) do not depend on morphometric properties. The results we obtained are mixed: there are four

subcatchments for which the scaling laws are verified and therefore all four GIUHs are similar and four subcatchments with some scaling laws verified with a majority of similar GIUHs. There are also for four subcatchments where a majority of scaling laws are not verified, and therefore the conditions for the calculation of  $G_N$  and  $G_{Ne}$  are not met.

Scaling laws, morphometric descriptors and GIUHs are still not extensively used in urban hydrology. A major result of this work is to apply a methodology widely used on natural networks for applications on urban CSS networks. The major difficulties are related to the uncertainties in the identification of the urban CSS network, the calculation of the upstream drained area for each pixel, and the non-verification of certain scaling laws. However, despite the difficulties encountered, the primary results are encouraging and open many perspectives for applications. This section discusses the practical use of morphometric descriptors in urban areas, and their wider use in urban hydrological modelling.

## 5.1 | Practical use of morphometric descriptors in urban areas

The methodology put forward in this work involves three steps: (i) selection of catchments; (ii) calculation of morphometric descriptors; (iii) calculation of the hydrological signatures of the GIUHs.

To illustrate the methodology developed in this work, we have chosen the network of the Parisian region which has largely evolved over the last two centuries. This choice is based on the network's unique structure. Twelve subcatchments were selected to illustrate the methodology on a large number of sites, and to show a possible spatial variability of the morphometric descriptors. It is obvious that the numerical values of the descriptors and the corresponding GIUHs are specific to each catchment, but some properties of scale invariance and the range of variation of the descriptors could be considered as characteristic of this type of urban network and therefore transposable to other similar networks. Note that for other applications on urban areas, the catchment outlet can be also be set at the right of certain installations, namely storm overflows or lifting stations, which constitute points of discontinuity for the network.

The methodology proposed in this work uses as an example, three categories of scaling laws (Horton-Strahler, Rodríguez-Iturbe and Moussa-Bocquillon) and their corresponding morphometric descriptors. However, many descriptors have been proposed in the literature such as Hack's law, Gravelius, Tokunaga, etc. and others more adapted to the complexity of urban zones (Gudmundsson & Mohajeri, 2013) can be easily added. These descriptors were largely used for channel network comparison and classification (Moussa, 2008, 2009). However, they depend on the channel network topology. On natural catchments, Digital Elevation Models (DEMs) are generally used to automatically extract the channel network using various algorithms. The extracted channel network will depend on the type of the DEM and the method used to extract it. In urban areas, the problem becomes more complex because the network does not necessarily follow the topography and certain parts of the network are not mapped.

Gironás et al. (2009) proposed a method using the DEM but constrained it by the urban network, which is true for the stormwater network. Recently, Blumensaat et al. (2012), Allard (2015), Lagesse (2015), Chahinian et al. (2019) and Chancibault et al. (2020) proposed new and original algorithms to identify urban networks that are often located under the street network. Improving methods for identifying and mapping the sewer network is a major challenge for obtaining better quality data in urban areas. Finally, morphometric descriptors can be used for generating virtual channel networks in urban areas. Simulating urban hydrology using actual sewer networks can be tedious. Therefore, the rapid generation of artificial networks is of considerable interest. Ghosh et al. (2006) present an application for generating artificial sewer networks using the dendritic and space filling 'Tokunaga' fractal tree geometry, Bonnet (2009) proposes a model to simulate channel network genesis and landscape erosion, and Borse and Biswal (2023) a model to explain river network evolution.

The GIUHs can be considered as hydrological signatures characterizing the channel network's hydrological response during flood events. In this work four GIUHs were compared: the Width Function, the Nash, the Nash equivalent and the Hayami formulations. Additional GIUHs could be easily added and compared. The GIUH represents the catchment response to a unit rainfall. The simplest and most widely used assumption assumes spatially uniform rain and a uniform runoff coefficient. This approach has been extended to represent variable rainfall in space (Moussa, 2008) or to take into account the spatial variability of rainfall and the runoff coefficient (Andrieu et al., 2021). These new approaches allow the calculation of GIUHs taking into account the spatial variability of rainfall and land cover, and thus make it possible to test the impact of future scenarios of change in rainfall or land use. Moreover, little physical evidence exists on how such signatures change in time as a function of drainage network evolution. For example, Bennett and Liu (2016) studied rill genesis using morphometric properties such as Hack's law evolution once the network began to grow, Cheraghi et al. (2018) studied the properties of channel networks with time evolution during a laboratory experiment and Jovanovic et al. (2019) calculated network properties depicting the urban development and stormwater network at different times. Finally, given that the GIUH can be considered as a "probability density function", this methodology can be extended by replacing the upstream drained area by the quantity corresponding to the variable of interest (i.e., pollutants, sediments, number of inhabitants, etc.).

## 5.2 | Application in urban hydrological modelling

Morphometric descriptors have been integrated into some hydrological models used on natural catchment (Jeffers & Montalto, 2018), but very few applications have been carried out in urban areas. For example, Biswal and Marani (2010) and Biswal and Kumar (2013) studied the link between morphometric descriptors and key recession curves properties through a conceptual geomorphological recession flow model. Di Lazaro and Volpi (2011) modelled the effects of hillslope dynamics and network geometry on the scaling properties of the hydrologic response.

Incorporating channel network morphology into stream modelling using GIUHs is also a well-accepted scientific practice now in hydrological modelling. However, very few attempts have been made so far to use channel networks for modelling total flow, not just flood flow. Recently, Biswal and Singh (2017) proposed to model the total flow partitioned into surface flow and subsurface flow, which are both then modelled separately by constructing channel network morphology based on GIUHs.

Finally, operational applications can be considered such as the design of urban infrastructure networks to enhance their resilience to external and internal threats (Krueger et al., 2017).

## 6 | CONCLUSIONS

While morphometric properties of channel networks, scaling laws and Geomorphological Instantaneous Unit Hydrographs (GIUHs) have been largely studied on natural channel networks which have the properties of Optimal Channel Networks (OCNs), very few applications were carried out on non-OCN artificial channel networks such as combined sewer networks in urban areas. Therefore, questions may rise as to whether the scaling laws established for OCNs may also be true for non-OCN sewer networks, and if these laws are verified, how they may impact the shape of the GIUHs?

In this work, applications were carried out on the CSS of the Greater Paris which was subdivided into 12 nested subcatchments. The Greater Paris CSS presents several specificities related to its evolution and extension during centuries, and its adaptation to the particular case of the city of Paris. In smaller towns location maps may be inaccurate or the network's topology, mainly node connectivity, may not be available for some areas. Hence, the sewer network topology is not easily available as it is the case for Digital Terrain Models and natural river networks. An important digitization work of the Greater Paris CSS was necessary and constitutes a primary step before any treatment of the morphometric properties.

A two-step methodology is put forward in this work. First, the morphometric properties are analysed using the reference Horton-Strahler, the power law of Rodriguez-Iturbe and the scaling laws of Moussa-Bocquillon. The results show that Horton-Strahler's law of bifurcation is generally verified while the two laws of length and areas are not verified for the majority of the twelve catchments. Moreover, the ratios  $R_B$ ,  $R_L$  and  $R_A$  are not in the same range of values as those of natural catchments. Rodriguez-Iturbe's scaling law is verified for all the catchments but with different values of the regression line slope which ranges between 0.4 and 0.5, in comparison to 0.43 for OCNs. Moussa-Bocquillon's laws of source nodes  $N(S)$  and total channel length  $T(S)$  are verified for a large majority of the twelve catchments with slightly different values of the descriptors in comparison to OCNs. Similar values are produced for Moussa-Bocquillon's  $U$  constant in comparison to OCNs but with high values of the coefficient of variation. Moreover, Moussa-Bocquillon's morphometric properties show stability for both OCNs and CSSs.

The second step uses these morphometric properties to calculate four Geomorphological Instantaneous Unit Hydrographs GIUHs: the reference Width Function ( $G_{WF}$ ), the Nash unit hydrograph ( $G_N$ ) using Horton-Strahler ratios, the equivalent Nash unit hydrograph ( $G_{Ne}$ ) which is an improvement of the previous one using Moussa-Bocquillon descriptors, and the Hayami function ( $G_H$ ) solution of the diffusive wave equation. When comparing the GIUHs, the  $G_{Ne}$ ,  $G_H$  and  $G_{WF}$  produce similar maximum value of the GIUH and time to peak values for the CSSs, unlike the  $G_N$  obtained using Horton-Strahler's ratios, whose response differs the most compared to the other three functions. The  $G_{Ne}$ 's response is very consistent when compared to the one obtained by the diffusive wave model and the width function, but is contrary to the  $G_N$ 's. Finally, we have identified four catchments for which the scaling laws are verified and therefore all GIUHs are similar. On the other hand, for four catchments the scaling laws are not verified and this strongly impacts the GIUHs.

This method's full potential has not been completely investigated yet. Indeed, the method can be extended to follow the evolution of a catchment over time and highlight the effect of urbanization on its response (Bunster et al., 2019). Furthermore, landuse can be better accounted for by spatially distributing the runoff coefficient for each pixel of the catchment or by relating it to the number of connected units in the case of agricultural or urban catchments. This method must be applied on a larger number of CSSs to verify its efficiency in the determination of the hydrological response of urban catchments. This would allow for a better anticipation of water and pollutant arrival times in case of combined sewer overflow and improved operation of wastewater treatment plants.

## ACKNOWLEDGEMENTS

The authors thank the French Research Institute for Sustainable Development (IRD) for financial support. The reconstructed network has been financially supported by the research program PIREN-Seine 7 and allowed by SIAAP and the management teams of the sewer network of Ville de Paris, Hauts-de-Seine, Seine-Saint-Denis and Val-de-Marne. The authors thank them for providing data and expertise.

The authors gratefully acknowledge the reviewers for their valuable comments. Their insightful observations and constructive criticism greatly enhanced the quality and depth of the research. The authors thank them for the time and effort they dedicated to providing such detailed and thoughtful comments.

## DATA AVAILABILITY STATEMENT

The data that support the findings of this study are available from Katia Chancibault (Univ Gustave Eiffel, GERS-LEE, F-44344 Bouguenais, France; [katia.chancibault@univ-eiffel.fr](mailto:katia.chancibault@univ-eiffel.fr)) upon reasonable request.

## ORCID

Mohamad Achour  <https://orcid.org/0009-0003-1309-8684>



## REFERENCES

- Albert, R., & Barabási, A. (2002). Statistical mechanics of complex networks. *Reviews of Modern Physics*, 74, 47–97. <https://doi.org/10.1103/RevModPhys.74.47>
- Allard, A. (2015). Contribution à la modélisation hydrologique à l'échelle de la ville Application sur la ville de Nantes. PhD, Université Nantes, Angers Le Mans – Ecole Centrale de Nantes. 223. <https://hal.science/tel-02380123>
- Andrieu, H., Moussa, R., & Kirstetter, P. E. (2021). The event-specific geomorphological instantaneous unit hydrograph (E-GIUH): The basin hydrological response characteristic of a flood event. *Journal of Hydrology*, 603, 127158. <https://doi.org/10.1016/j.jhydrol.2021.127158>
- Bamufleh, S., Al-Wagdany, A., Elfeki, A., & Chaabani, A. (2020). Developing a geomorphological instantaneous unit hydrograph (GIUH) using equivalent Horton-Strahler ratios for flash flood predictions in arid regions. *Geomatics, Natural Hazards and Risk*, 11(1), 1697–1723. <https://doi.org/10.1080/19475705.2020.1811404>
- Barabási, A. L., & Albert, R. (1999). Emergence of scaling laws in random networks. *Science*, 286, 509–512. <https://doi.org/10.1126/science.286.5439.509>
- Battin, T. J., Kaplan, L. A., Findlay, S., Hopkinson, C. S., Marti, E., Packman, A. I., Newbold, J. D., & Sabater, F. (2008). Biophysical controls on organic carbon fluxes in fluvial networks. *Nature Geoscience*, 1(2), 95–100. <https://doi.org/10.1038/ngeo101>
- Bennett, S. J., & Liu, R. (2016). Basin self-similarity, Hack's law, and the evolution of experimental rill networks. *Geology*, 44(1), 35–38. <https://doi.org/10.1130/G37214.1>
- Bertuzzo, E., Helton, A. M., Hall, R. O., & Battin, T. J. (2017). Scaling of dissolved organic carbon removal in river networks. *Advances in Water Resources*, 110, 136–146. <https://doi.org/10.1016/j.advwatres.2017.10.009>
- Biswal, B., & Kumar, D. N. (2013). A general geomorphological recession flow model for river basins. *Water Resources Research*, 49, 4900–4906. <https://doi.org/10.1002/wrcr.20379>
- Biswal, B., & Marani, M. (2010). Geomorphological origin of recession curves. *Geophysical Research Letters*, 37, L24403. <https://doi.org/10.1029/2010GL045415>
- Biswal, B., & Singh, R. (2017). Incorporating channel network information in hydrologic response modelling: Development of a model and inter-model comparison. *Advances in Water Resources*, 100, 168–182. <https://doi.org/10.1016/j.advwatres.2016.12.015>
- Blumensaat, F., Wolfram, M., & Krebs, P. (2012). Sewer model development under minimum data requirements. *Environmental Earth Sciences*, 65, 1427–1437. <https://doi.org/10.1007/s12665-011-1146-1>
- Bonnet, S. (2009). Shrinking and splitting of drainage basins in orogenic landscapes from the migration of the main drainage divide. *Nature Geoscience*, 2, 766–771. <https://doi.org/10.1038/ngeo666>
- Borse, B., & Biswal, B. (2023). A novel probabilistic model to explain drainage network evolution. *Advances in Water Resources*, 171, 104342. <https://doi.org/10.1016/j.advwatres.2022.104342>
- Botturi, A., Ozbayram, E. G., Tondera, K., Gilbert, N. I., Rouault, P., Caradot, N., Gutierrez, O., Daneshgar, S., Frison, N., Akyol, Ç., Foglia, A., Eusebi, A. L., & Fatone, F. (2021). Combined sewer overflows: A critical review on best practice and innovative solutions to mitigate impacts on environment and human health. *Critical Reviews in Environmental Science and Technology*, 51(15), 1585–1618. <https://doi.org/10.1080/10643389.2020.1757957>
- Bunster, T., Gironás, J., & Niemann, J. D. (2019). On the influence of upstream flow contributions on the basin response function for hydrograph prediction. *Water Resources Research*, 55(6), 4915–4935. <https://doi.org/10.1029/2018WR024510>
- Burian, S. J., Nix, S. J., Pitt, R. E., & Durrans, S. R. (2000). Urban wastewater Management in the United States: Past, Present, and Future. *Journal of Urban Technology*, 7(3), 33–62. <https://doi.org/10.1080/713684134>
- Chahinian, N., Delenne, C., Commandré, B., Derras, M., Deruelle, L., & Bailly, J.-S. (2019). Automatic mapping of urban wastewater networks based on manhole cover locations. *Computers, Environment and Urban Systems*, 78, 101370. <https://doi.org/10.1016/j.compenvurbysys.2019.101370>
- Chancibault, K., Mosset, A., Lotfi, Z., Shobair, S., Lehoucq, C., Azimi, S., Rocher, V., Bernard, E., Chebbo, G., & Andrieu, H. (2020). Reconstruction and simplification of the greater Paris sewerage network. *Seconde International Conference "Water, Megacities and Global Change" - Online Pre-conference*, Dec 2020, Online, France. 11. [hal-03120431v2](https://hal.archives-ouvertes.fr/hal-03120431v2) <https://hal.archives-ouvertes.fr/hal-03120431/document>
- Cheraghi, M., Rinaldo, A., Sander, G. C., Perona, P., & Barry, D. A. (2018). Catchment drainage network scaling laws found experimentally in overland flow morphologies. *Geophysical Research Letters*, 45, 9614–9622. <https://doi.org/10.1029/2018GL078351>
- Chow, V. T., Maidment, D. R., & Mays, L. W. (1988). *Applied hydrology*, McGraw-Hill, New York (ISBN-0-07-100174-3).
- Coble, A. A., Koenig, L. E., Potter, J. D., Parham, L. M., & McDowell, W. H. (2019). Homogenization of dissolved organic matter within a river network occurs in the smallest headwaters. *Biogeochemistry*, 143(1), 85–104. <https://doi.org/10.1007/s10533-019-00551-y>
- Courtat, T., Gloaguen, C., & Douady, S. (2011). Mathematics and morphogenesis of cities: A geometrical approach. *Physical Review E*, 83(3), 036106. <https://doi.org/10.1103/PhysRevE.83.036106>
- Di Lazzaro, M., & Volpi, E. (2011). Effects of hillslope dynamics and network geometry on the scaling properties of the hydrologic response. *Advances in Water Resources*, 34, 1496–1507. <https://doi.org/10.1016/j.advwatres.2011.07.012>
- Dietrich, W. E., Wilson, C. J., Montgomery, D. R., & McKean, J. (1993). Analysis of erosion thresholds, channel networks, and landscape morphology using a digital terrain model. *The Journal of Geology*, 101(2), 259–278. <https://doi.org/10.1086/648220>
- Dodds, P. S., & Rothman, D. H. (2000). Scaling, universality, and geomorphology. *Annual Review of Earth and Planetary Sciences*, 28(1), 571–610. <https://doi.org/10.1146/annurev.earth.28.1.571>
- Ghosh, I., Hellweger, F. L., & Fritsch, T. G. (2006). Fractal generation of artificial sewer networks for hydrologic simulations. *Proceedings of the 2006 ESRI International user Conference*. 1–25.
- Gires, A., Abbes, J. B., da Silva Rocha Paz, I., Tchiguirinskaia, I., & Schertzer, D. (2018). Multifractal characterisation of a simulated surface flow: A case study with multi-hydro in Jouy-en-Josas, France. *Journal of Hydrology*, 558, 482–495. <https://doi.org/10.1016/J.JHYDROL.2018.01.062>
- Gires, A., Giangola-Murzyn, A., Abbes, J. B., Tchiguirinskaia, I., Schertzer, D., & Lovejoy, S. (2015). Impacts of small scale rainfall variability in urban areas: A case study with 1D and 1D/2D hydrological models in a multifractal framework. *Urban Water Journal*, 12(8), 607–617. <https://doi.org/10.1080/1573062x.2014.923917>
- Gires, A., Tchiguirinskaia, I., Schertzer, D., Ochoa-Rodriguez, S., Willems, P., Ichiba, A., Wang, L.-P., Pina, R., van Assel, J., Bruni, G., Murla Tuyls, D., & ten Veldhuis, M.-C. (2017). Fractal analysis of urban catchments and their representation in semi-distributed models: Imperviousness and sewer system. *Hydrology and Earth System Sciences*, 21(5), 2361–2375. <https://doi.org/10.5194/hess-21-2361-2017>
- Gironás, J., Niemann, J. D., Roesner, L. A., Rodriguez, F., & Andrieu, H. (2009). A morpho-climatic instantaneous unit hydrograph model for urban catchments based on the kinematic wave approximation. *Journal of Hydrology*, 377(3–4), 317–334. <https://doi.org/10.1016/j.jhydrol.2009.08.030>
- Gudmundsson, A., & Mohajeri, N. (2013). Entropy and order in urban street networks. *Science Report*, 3, 3324. <https://doi.org/10.1038/srep03324>
- Gupta, V. K., Waymire, E., & Wang, C. T. (1980). A representation of an instantaneous unit hydrograph from geomorphology. *Water*

- Resources Research*, 16(5), 855–862. <https://doi.org/10.1029/WR016i005p00855>
- Hallema, D. W., & Moussa, R. (2014). A model for distributed GIUH-based flow routing on natural and anthropogenic hillslopes. *Hydrological Processes*, 28(18), 4877–4895. <https://doi.org/10.1002/hyp.9984>
- Hayami, S. (1951). *On the propagation of flood waves*, 12–20. Kyoto Univ <http://hdl.handle.net/2433/123641>
- Horton, R. E. (1945). Erosional development of streams and their drainage basins: Hydrophysical approach to quantitative morphology. *Bulletin of the Geological Society of America*, 56, 2 75–3 70. <https://doi.org/10.1177/030913339501900406>
- Hrachowitz, M., Savenije, H. H. G., Blöschl, G., McDonnell, J. J., Sivapalan, M., Pomeroy, J. W., Arheimer, B., Blume, T., Clark, M. P., Ehret, U., Fenicia, F., Freer, J. E., Gelfan, A., Gupta, H. V., Hughes, D. A., Hut, R. W., Montanari, A., Pande, S., Tetzlaff, D., ... Cudennec, C. (2013). A decade of predictions in ungauged basins (PUB)-a review. *Hydrological Sciences Journal*, 58(6), 1198–1255. <https://doi.org/10.1080/02626667.2013.803183>
- Ibbitt, R. P. (1997). Evaluation of optimal channel network and river basin heterogeneity concepts using measured flow and channel properties. *Journal of Hydrology*, 196(1–4), 119–138. [https://doi.org/10.1016/S0022-1694\(96\)03293-3](https://doi.org/10.1016/S0022-1694(96)03293-3)
- Jeffers, S., & Montalto, F. (2018). Modeling urban sewers with artificial fractal geometries. *Journal of Water Management Modeling*, 26, C455. <https://doi.org/10.14796/JWMM.C455>
- Jovanovic, T., Hale, R. L., Gironás, J., & Mejía, A. (2019). Hydrological functioning of an evolving urban Stormwater network. *Water Resources Research*, 55(8), 6517–6533. <https://doi.org/10.1029/2019WR025236>
- Kim, J. C. (2022). Equivalent Horton's ratios of channel network within the framework of variable source basin area. *Journal of Hydrology: Regional Studies*, 39, 100994. <https://doi.org/10.1016/j.ejrh.2022.100994>
- Kirkby, M. J. (1976). Tests of the random network model, and its application to basin hydrology. *Earth Surface Processes*, 1(3), 197–212. <https://doi.org/10.1002/esp.3290010302>
- Krueger, E., Klinkhamer, C., Urich, C., Zhan, X., & Rao, P. S. C. (2017). Generic patterns in the evolution of urban water networks: Evidence from a large Asian city. *Physical Review E*, 95(3), 032312. <https://doi.org/10.1103/PhysRevE.95.032312>
- Kvitsjøen, J., Paus, K. H., Bjerkholt, J. T., Fergus, T., & Lindholm, O. (2021). Intensifying rehabilitation of combined sewer systems using trenchless technology in combination with low impact development and green infrastructure. *Water Science and Technology*, 83(12), 2947–2962. <https://doi.org/10.2166/wst.2021.198>
- Lagesse, C. (2015). *Lire les Lignes de la Ville: Méthodologie de caractérisation des graphes spatiaux*. Géographie. PhD, University Paris Diderot-Paris VII, France. 566. <https://shs.hal.science/tel-01245898>
- Laroulandie, F. (1993). Les égouts de Paris au XIXe siècle: l'enfer vaincu et l'utopie dépassée. *Cahiers de Fontenay, n° 69–70, Idées de villes, villes idéales*. 107–140 <https://doi.org/10.3406/cafon.1993.1614>
- Martinez, C., Hancock, G. R., Kalma, J. D., Wells, T., & Boland, L. (2010). An assessment of digital elevation models and their ability to capture geomorphic and hydrologic properties at the catchment scale. *International Journal of Remote Sensing*, 31(23), 6239–6257. <https://doi.org/10.1080/01431160903403060>
- Masucci, A. P., Stanilov, K., & Batty, M. (2014). Exploring the evolution of London's street network in the information space: A dual approach. *Physical Review E*, 89(1), 012805. <https://doi.org/10.1103/PhysRevE.89.012805>
- McGrath, G., Kaeseberg, T., Reyes Silva, J. D., Jawitz, J. W., Blumensaat, F., Borchardt, D., Mellander, P. E., Paik, P., Krebs, P., & Rao, P. S. C. (2019). Network topology and rainfall controls on the variability of combined sewer overflows and loads. *Water Resources Research*, 55, 9578–9591. <https://doi.org/10.1029/2019WR025336>
- Meierdiercks, K. L., Smith, J. A., Baeck, M. L., & Miller, A. J. (2010). Analyses of urban drainage network structure and its impact on hydrologic response. *Journal of the American Water Resources Association*, 46(5), 932–943. <https://doi.org/10.1111/j.1752-1688.2010.00465.x>
- Moussa, R. (1997). Geomorphological transfer function calculated from digital elevation models for distributed hydrological modelling. *Hydrological Processes*, 11(5), 429–449. [https://doi.org/10.1002/\(SICI\)1099-1085\(199704\)11:5<429::AID-HYP471>3.0.CO;2-J](https://doi.org/10.1002/(SICI)1099-1085(199704)11:5<429::AID-HYP471>3.0.CO;2-J)
- Moussa, R. (2003). On morphometric properties of basins, scale effects and hydrological response. *Hydrological Processes*, 17(1), 33–58. <https://doi.org/10.1002/hyp.1114>
- Moussa, R. (2008). What controls the width function shape, and can it be used for channel network comparison and regionalization? *Water Resources Research*, 44(8), 1–19. <https://doi.org/10.1029/2007WR006118>
- Moussa, R. (2009). Definition of new equivalent indices of Horton-Strahler ratios for the derivation of the geomorphological instantaneous unit hydrograph. *Water Resources Research*, 45(9), W09406. <https://doi.org/10.1029/2008WR007330>
- Moussa, R., & Bocquillon, C. (1993). Morphologie fractale du réseau hydrographique. *Hydrological Sciences Journal IAHS*, 38(3), 187–201.
- Moussa, R., & Bocquillon, C. (1996). Fractal analysis of tree-like channel network from digital elevation model. *Journal of Hydrology*, 187, 157–172. [https://doi.org/10.1016/S0022-1694\(96\)03093-4](https://doi.org/10.1016/S0022-1694(96)03093-4)
- Moussa, R., Colin, F., & Rabotin, M. (2011). Invariant morphometric properties of headwater subcatchments. *Water Resources Research*, 47(8), 1–15. <https://doi.org/10.1029/2010WR010132>
- Muneepeerakul, R., Bertuzzo, E., Rinaldo, A., & Rodriguez-Iturbe, I. (2019). Evolving biodiversity patterns in changing river networks. *Journal of Theoretical Biology*, 462, 418–424. <https://doi.org/10.1016/j.jtbi.2018.11.021>
- Munro, K., Martins, C. P. B., Loewenthal, M., Comber, S., Cowan, D. A., Pereira, L., & Barron, L. P. (2019). Evaluation of combined sewer overflow impacts on short-term pharmaceutical and illicit drug occurrence in a heavily urbanised tidal river catchment (London, UK). *Science of the Total Environment*, 657, 1099–1111. <https://doi.org/10.1016/j.scitotenv.2018.12.108>
- Nash, J. E. (1957). The form of the instantaneous unit hydrograph, IAHS Publ. 42. 114–118.
- Nickel, J. P., & Fuchs, S. (2019). Micropollutant emissions from combined sewer overflows. *Water Science and Technology*, 80(11), 2179–2190. <https://doi.org/10.2166/wst.2020.035>
- O'Callaghan, J. F., & Mark, D. M. (1984). The extraction of drainage networks from digital elevation data. *Computer Vision, Graphics, and Image Processing*, 28(3), 323–344. [https://doi.org/10.1016/S0734-189X\(84\)80011-0](https://doi.org/10.1016/S0734-189X(84)80011-0)
- Paik, K., & Kumar, P. (2008). Emergence of self-similar tree network organization. *Complexity*, 13(4), 30–37. <https://doi.org/10.1002/cplx.20214>
- Raff, D. A., Smith, J. L., & Trlica, M. J. (2003). Statistical descriptions of channel networks and their shapes on non-vegetated hillslopes in Kemmerer, Wyoming. *Hydrological Processes*, 17(10), 1887–1897. <https://doi.org/10.1002/hyp.1216>
- Reid, D. (1993). *Paris sewers and Sewermen: Realities and representations* (1st ed.). Harvard University Press.
- Rigon, R., Bancheri, M., Formetta, G., & deLavenne, A. (2016). The geomorphological unit hydrograph from a historical-critical perspective. *Earth Surface Processes and Landforms*, 41(1), 27–37. <https://doi.org/10.1002/esp.3855>
- Rigon, R., Rinaldo, A., Rodriguez-Iturbe, I., Bras, R. L., & Ijjasz-Vasquez, E. (1993). Optimal channel networks: A framework for the study of river basin morphology. *Water Resources Research*, 29(6), 1635–1646. <https://doi.org/10.1029/92WR02985>
- Rinaldo, A., Rodriguez-Iturbe, I., Rigon, R., Bras, R. L., Ijjasz-Vasquez, E., & Marani, A. (1992). Minimum energy and fractal structures of drainage networks. *Water Resources Research*, 28(9), 2183–2195. <https://doi.org/10.1029/92WR00801>

- Rodríguez, F., Cudennec, C., & Andrieu, H. (2005). Application of morphological approaches to determine unit hydrographs of urban catchments. *Hydrological Processes*, 19(5), 1021–1035. <https://doi.org/10.1002/hyp.5643>
- Rodríguez-Iturbe, I., Caylor, K. K., & Rinaldo, A. (2011). Metabolic principles of river basin organization. *Proceedings of the National Academy of Sciences*, 108(29), 11751–11755. <https://doi.org/10.1073/pnas.1107561108>
- Rodríguez-Iturbe, I., Devoto, G., & Valdés, J. B. (1979). Discharge response analysis and hydrologic similarity: The interrelation between the geomorphologic IUH and the storm characteristics. *Water Resources Research*, 15(6), 1435–1444. <https://doi.org/10.1029/WR015i006p01435>
- Rodríguez-Iturbe, I., Ijjász-Vasquez, E., Bras, R. L., & Tarboton, D. G. (1992). Power-law distribution of mass and energy in river basins. *Water Resources Research*, 28(4), 1089–1093. <https://doi.org/10.1029/91WR03033>
- Rodríguez-Iturbe, I., Muneeppeerakul, R., Bertuzzo, E., Levin, S. A., & Rinaldo, A. (2009). River networks as ecological corridors: A complex systems perspective for integrating hydrologic, geomorphologic, and ecologic dynamics. *Water Resources Research*, 45(1), W01413. <https://doi.org/10.1029/2008WR007124>
- Rodríguez-Iturbe, I., & Rinaldo, A. (1997). *Fractal River basins: Chance and self-organization*. Cambridge University Press.
- Rodríguez-Iturbe, I., Rinaldo, A., Rigon, R., Bras, R. L., Marani, A., & Ijjász-Vásquez, E. (1992). Energy dissipation, runoff production, and the three-dimensional structure of river basins. *Water Resources Research*, 28(4), 1095–1103. <https://doi.org/10.1029/91WR03034>
- Rodríguez-Iturbe, I., & Valdés, J. B. (1979). The geomorphologic structure of hydrologic response. *Water Resources Research*, 15(6), 0043–1397. <https://doi.org/10.1029/WR015i006p01409>
- Rossel, F., Gironás, J., Mejía, A., Rinaldo, A., & Rodríguez, F. (2014). Spatial characterization of catchment dispersion mechanisms in an urban context. *Advances in Water Resources*, 74, 290–301. <https://doi.org/10.1016/j.advwatres.2014.09.005>
- Rosso, R. (1984). Nash model relation to Horton order ratios. *Water Resources Research*, 20(7), 914–920. <https://doi.org/10.1029/WR020i007p00914>
- Saco, P. M., & Kumar, P. (2002a). Kinematic dispersion in stream networks: 1. Coupling hydraulic and network geometry. *Water Resources Research*, 38(11), 26-1–26-14. <https://doi.org/10.1029/2001wr000695>
- Saco, P. M., & Kumar, P. (2002b). Kinematic dispersion in stream networks: 2. Scale issues and self-similar network organization. *Water Resources Research*, 38(11), 27-1–27-15. <https://doi.org/10.1029/2001wr000694>
- Seybold, H., Rothman, D. H., & Kirchner, J. W. (2017). Climate's watermark in the geometry of stream networks. *Geophysical Research Letters*, 44, 2272–2280. <https://doi.org/10.1002/2016GL072089>
- Smart, J. (1969). Topological properties of channel networks. *GSA Bulletin*, 80(9), 1757–1774. [https://doi.org/10.1130/0016-7606\(1969\)80\[1757:TPOCN\]2.0.CO;2](https://doi.org/10.1130/0016-7606(1969)80[1757:TPOCN]2.0.CO;2)
- Strahler, A. N. (1957). Quantitative analysis of watershed geomorphology. *Eos, Transactions American Geophysical Union*, 38(6), 913–920. <https://doi.org/10.1029/TR038i006p00913>
- Tarboton, D. G. (1996). Fractal river networks, Horton's laws and Tokunaga cyclicity. *Journal of Hydrology*, 187(1–2), 105–117. [https://doi.org/10.1016/S0022-1694\(96\)03089-2](https://doi.org/10.1016/S0022-1694(96)03089-2)
- Tarboton, D. G., & Ames, D. P. (2004). Advances in the mapping of flow networks from digital elevation data. *Bridging the Gap: Meeting the World's Water and Environmental Resources Challenges - Proceedings of the World Water and Environmental Resources Congress, 2001*, 111. [https://doi.org/10.1061/40569\(2001\)166](https://doi.org/10.1061/40569(2001)166)
- Tokunaga, E. (1978). Consideration on the composition of drainage networks and their evolution. *Geographical Reports of Tokyo Metropolitan University*, No. 13.
- Wollheim, W. M., Bernal, S., Burns, D. A., Czuba, J. A., Driscoll, C. T., Hansen, A. T., Hensley, R. T., Hosen, J. D., Inamdar, S., Kaushal, S. S., Koenig, L. E., Lu, Y. H., Marzadri, A., Raymond, P. A., Scott, D., Stewart, R. J., Vidon, P. G., & Wohl, E. (2018). River network saturation concept: Factors influencing the balance of biogeochemical supply and demand of river networks. *Biogeochemistry*, 141(3), 503–521. <https://doi.org/10.1007/s10533-018-0488-0>
- Yang, S., Paik, K., McGrath, G. S., Urlich, C., Krueger, E., Kumar, P., & Rao, P. S. C. (2017). Functional topology of evolving urban drainage networks. *Water Resources Research*, 53(11), 8966–8979. <https://doi.org/10.1002/2017WR021555>
- Zischg, J., Klinkhamer, C., Zhan, X., Rao, P. S. C., & Sitzenfrie, R. (2019). A century of topological coevolution of complex infrastructure networks in an Alpine City. *Complexity*, 2019, 1–16. <https://doi.org/10.1155/2019/2096749>

## SUPPORTING INFORMATION

Additional supporting information can be found online in the Supporting Information section at the end of this article.

**How to cite this article:** Achour, M., Chahinian, N., Chancibault, K., Andrieu, H., & Moussa, R. (2023). Morphometric properties, scaling laws and hydrologic response of the Greater Paris combined sewer system. *Hydrological Processes*, 37(10), e14984. <https://doi.org/10.1002/hyp.14984>

## APPENDIX A: LIST OF NOTATIONS

- $A_w$ : mean area contributing to streams of order  $w$  and its tributary ( $1 \leq w \leq \Omega$ ) (Equation 3).
- $b$ : parameter in Moussa-Bocquillon law  $T(S)$  (Equation 6).
- CSS: combined sewer system.
- $D$ : dispersion (Equation 12).
- GIUH: Geomorphologic Instantaneous Unit Hydrograph.
- $G_N$ : Nash unit hydrograph.
- $G_{Ne}$ : Nash unit hydrograph equivalent.
- $G_H$ : Hayami function based GIUH.
- $G_{WF}$ : Width Function based GIUH.
- $g_p$ : Maximum value of the GIUH.
- $\bar{L}$ : mean length of distances from each pixel in a catchment to the outlet (Equation 11).
- $L_w$ : mean length of streams of order  $w$  (Equation 2).
- $L_\Omega$ : length of the channel of order  $\Omega$ .
- $m_1$ : parameter in Moussa-Bocquillon law  $T(S)$ , corresponding to  $m_1 = T(S_1)$  (Equation 6).
- $N(S)$ : Moussa-Bocquillon law of number of source catchments (Equation 5).

- $N_w$ : number of streams of order  $w$  (Equation 1).  
 non-OCN: non Optimal Channel Network.  
 OCN: Optimal Channel Network.  
 $R_A$ : Horton-Strahler area ratio (Equation 3).  
 $R_B$ : Horton-Strahler bifurcation ratio (Equation 1).  
 $R_L$ : Horton-Strahler length ratio (Equation 2).  
 $S$ : threshold area of upstream catchments used in Moussa-Bocquillon laws (Equations 5, 6 and 7).  
 $S_1$ : threshold area such as the number of source catchments  $N(S_1) = 1$  and  $N(S_1 - \epsilon) = 2$  (Equation 6).  
 $S_0$ : catchment area (Equations 5, 6 and 7).  
 $T_G$ : time of occurrence of the centre of gravity of the GIUH.  
 $T_p$ : time of occurrence of maximum value of the GIUH.  
 $T(S)$ : Moussa-Bocquillon law of channel network total length (Equation 6).  
 $v$ : velocity (Equation 9 and 11).  
 $w$ : order of the channel network following the Horton-Strahler classification.  
 $\alpha$ : parameter in Moussa-Bocquillon law  $N(S)$  (Equation 5).  
 $\beta$ : parameter in Rodriguez-Iturbe power law (Equation 4).  
 $\Gamma$ : gamma function (Equation 8).  
 $\lambda$ : parameter in Moussa-Bocquillon law  $N(S)$  (Equation 5).  
 $\Omega$ : magnitude or largest stream order.

## APPENDIX B: PROCEDURE TO EXTRACT THE NETWORK CHARACTERISTICS OF THE GREATER PARIS CSS

Geographic Information Systems offer many functionalities to extract the hydrographic network from Digital Elevation Models (DEM) using the D8 algorithm (O'Callaghan & Mark, 1984; Tarboton & Ames, 2004; Tarboton et al., 1991). However, the network in urban areas cannot be extracted from the DEM, and the flow does not follow the greatest slope at the ground surface. For this, we have developed specific procedures using functions available both in commercial and open-source GIS systems.

To compute the above morphometric descriptors and the GIUHs of a natural or urban catchment, a script based on ArcGIS 10.8 functions and coded in Python is developed. The first step consists in defining the catchment and identifying its hydrographic network. In the case of natural catchments, these two tasks are carried out using the ArcHydro library functions and a DEM. In the case of the Greater Paris combined sewer system, the database provides the catchments that correspond to each subcatchment and its network.

Through these files (network and catchment) the main raster is extracted: it is the raster of directions as defined by the D8 principle. This raster is obtained through the "Euclidean back direction" function, implemented in ArcGIS, which allows sending each cell to the nearest junction of the network by assigning it a direction value in degrees. Then these directions are modified into D8 form (each cell can be drained to a single upstream cell according to 8 drainage directions) so that this file is compatible with the ArcHydro library that is then used to extract the morphological and hydrological properties.

Regarding the Horton-Strahler laws, the classification is done manually, and the numbers, lengths, and drained areas of each stream order are calculated in the attribute table of the network. Then Equations (1), (2) and (3) are computed in Python to draw the graphs and extract the Horton Strahler parameters ( $R_B$ ,  $R_L$ , and  $R_A$ ).

To classify the internal and external nodes, and to calculate the geomorphological relationships (number of external points and total length of the network for a given threshold area), a loop of iterations is created, which takes as a hypothesis a value of threshold area and extracts the cells of the network that are able to drain at least this value through the "Stream Definition" from ArcHydro tools and then calculates the total length of the resulting network and the number of external points by using the "Data management" library of ArcGIS. Based on these results, the three graphs corresponding to Equations (4), (5) and (6) are generated and the equivalent Strahler parameters are determined (Equation 10).

In order to verify the power law, the raster of the accumulated drained surfaces must be calculated. The "Flow accumulation" function of ArcHydro is used to generate this raster using as input the raster of the drainage direction and the shapefile of the drainage network. In the attribute table of this raster, we find the number of cells that drain a specific area. This table is transformed into a list in python, and then the graph corresponding to the probability that a catchment cell drains at least a specific surface is generated and the slope of the curve ( $\Theta$ ) corresponding to the power law is calculated.

For the width function, the flow distance function is used, which assigns a value for the distance to the outlet for each cell. The generated raster data are then used to calculate the normalized width function and also the diffusion parameter (Equation 12 for the Hayami Equation 11).

This catchment property has been determined by the Flow Distance function in ArcMap. The normalized width function ( $G_{WF}$ ) (its integral is unitary) is represented as a function of time to compare the resulting catchment response to the other three GIUHs (Figure 6).